

# Responsive Magnetic Nanocomposites for Intelligent Shape-Morphing Microrobots

Yuan Liu, Gungun Lin,\* Mariana Medina-Sánchez,\* Maria Guix, Denys Makarov, and Dayong Jin\*



Cite This: *ACS Nano* 2023, 17, 8899–8917



Read Online

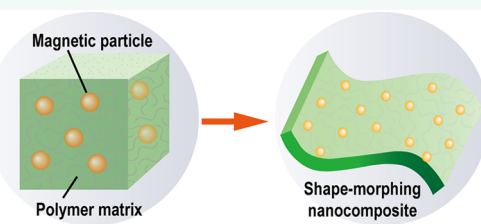
ACCESS |

Metrics & More

Article Recommendations

**ABSTRACT:** With the development of advanced biomedical theragnosis and bioengineering tools, smart and soft responsive microstructures and nanostructures have emerged. These structures can transform their body shape on demand and convert external power into mechanical actions. Here, we survey the key advances in the design of responsive polymer-particle nanocomposites that led to the development of smart shape-morphing microscale robotic devices. We overview the technological roadmap of the field and highlight the emerging opportunities in programming magnetically responsive nanomaterials in polymeric matrixes, as magnetic materials offer a rich spectrum of properties that can be encoded with various magnetization information. The use of magnetic fields as a tether-free control can easily penetrate biological tissues. With the advances in nanotechnology and manufacturing techniques, microrobotic devices can be realized with the desired magnetic reconfigurability. We emphasize that future fabrication techniques will be the key to bridging the gaps between integrating sophisticated functionalities of nanoscale materials and reducing the complexity and footprints of microscale intelligent robots.

**KEYWORDS:** Magnetic nanocomposites, Shape-morphing, Microrobots, Magnetic reconfigurability, Stimuli-responsive materials, Scalable manufacturing approaches, Soft materials, Biomedical and bioengineering applications



Microrobots are the next generation of microscale systems processing intriguing functionalities, with sizes typically in the range of a few microns to submillimeters. Such systems are comparable in size with biological cells, tissues, and human cavitory structures (e.g., gastrointestinal and blood circulatory systems), which makes them suitable for performing tasks that require the delicate manipulation of small biological entities and at locations that are often hard to reach by human beings.<sup>1–4</sup> Microrobots may also interact with molecules and cellular and tissue samples, in which the effective transduction of mechanical forces/torques is critical for not only controlling biophysical processes but also for clinical theragnostic applications.<sup>5–13</sup>

Despite significant progress, the development of microrobots is still inadequate for biomedical and bioengineering applications. First, the delivery and transport of microrobots *in vivo* is challenging because the internal biological environment is complex and has hierarchical terrains. The challenge requires a system that can closely mimic the capabilities of biological systems for performing multimodal locomotion (e.g., jumping, crawling, tumbling, etc.) to adapt to the complex environment. Several studies have assessed chemical fuel<sup>14</sup> for self-propulsion or external field control to facilitate greater dynamic maneuverability.<sup>15–19</sup> However, there is a mismatch between the size of the microrobots being designed and the

size of the systems that are required. Because of the unavailability of advanced manufacturing approaches, researchers have compromised on functional materials and the desired functionalities that need to be achieved. The integration of multiple functions in a small system and biocompatibility are major challenges that need to be overcome for the efficient functioning of such systems.<sup>20</sup> Second, the mechanical properties of biological specimens are highly heterogeneous, with stiffness ranging from 11 Pa (intestinal mucus) to 6.2 MPa (cartilage).<sup>21</sup> Traditional rigid systems are unsuitable for soft biological samples and living organisms. Additionally, rigid systems have very limited mechanical modes and are relatively large (in the submillimeter range and above), which limits their use in biomedical scenarios involving considerably smaller cavities, including blood vessels and intracellular spaces. To address the above challenges, many researchers have studied active nanomaterials in the presence of soft (polymeric) matrices and external stimuli, including light,<sup>22,23</sup> heat,<sup>24,25</sup>

Received: February 18, 2023

Accepted: April 26, 2023

Published: May 4, 2023



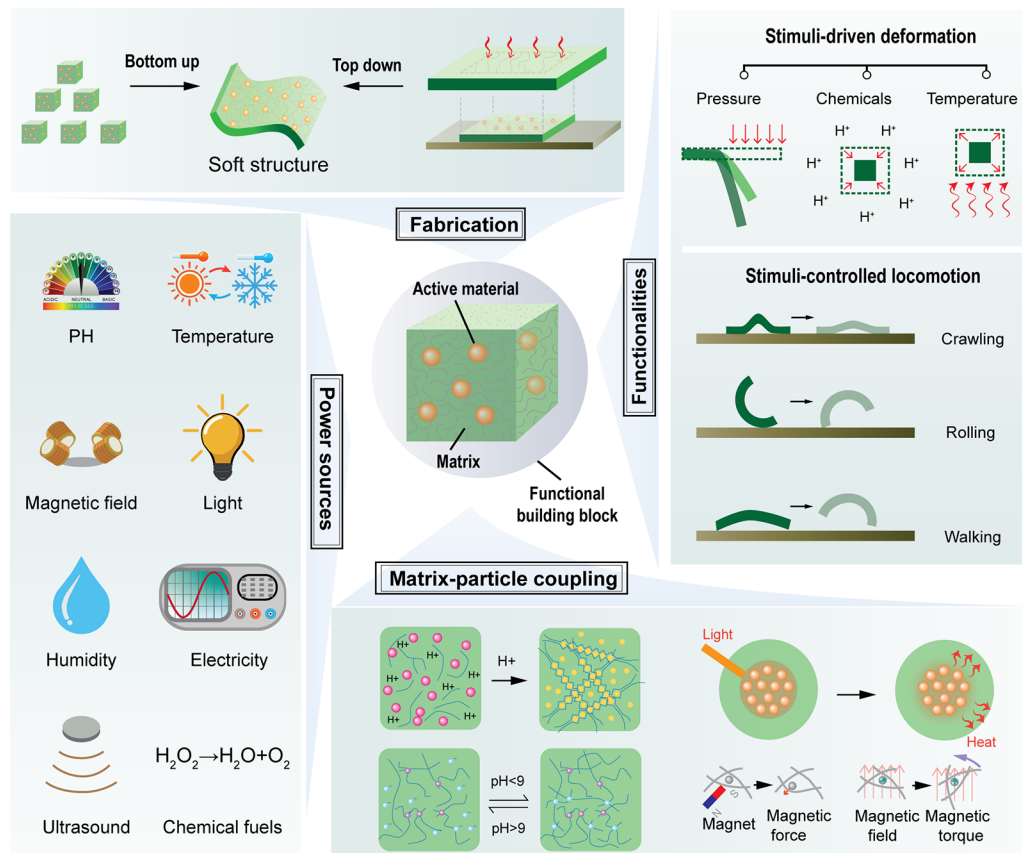


Figure 1. Landscape of developing soft and smart microrobots by designing responsive polymer–particle nanocomposites.

Table 1. Comparison of Various Actuation Mechanisms for Small-Scale Robots

power sources	propulsion mechanisms	key features	limitations
chemical solution <sup>49,50</sup>	- bubble propulsion - self-diffusiophoresis	- high motion speed (up to $10^3$ body length)	- solution-consuming process - uncontrollable motion - specific chemical fuels
microorganism <sup>45,51</sup>	biohybrid propulsion	- on-board sensing, actuation, and control functionalities	- fabrication efficiency - swarm coordinating - motion tracking - immune reactions
temperature <sup>52,53</sup>	thermal gradient	- no external stimulus required - ease of implementation	- limited to certain organs - may cause tissue damage
acoustic field <sup>54,55</sup>	- acoustic radiation force - acoustic streaming	- biocompatibility  - untethered manipulation - deep-tissue penetration capability	- biological sample damage due to local heating
light <sup>39,56</sup>	- local heating - shape morphing	- high-resolution spatial and temporal control - remote manipulation  - nontoxic and noninvasive physical field actuation	- cause tissue damage due to local heating - low efficiency for operating large micromachines with several hundreds of micrometers - low penetration depth due to light absorption of tissue
magnetic field <sup>14,57</sup>	- rotating magnetic field - gradient magnetic field	- nontethered and contactless operations  - deep-tissue penetration capability - biocompatibility	- low power efficiency  - high-cost requirements for medical instrumentation - limited to magnetic responsive materials

electric field,<sup>26,27</sup> and magnetic field (Figure 1).<sup>28–31</sup> The fabrication of soft microrobots is featured with controlled bottom-up assembly to create or top-down etching of functional nanomaterials as the building blocks. Microrobots of various morphologies (e.g., needles,<sup>32</sup> helices,<sup>33</sup> grippers,<sup>34</sup> and tube)<sup>35</sup> can be developed to adopt various locomotion

environments. In regard to the functionalities, soft microrobots can undergo passive stimuli-driven deformation (e.g., pressure,<sup>36</sup> chemical,<sup>37,38</sup> and temperature),<sup>39</sup> which can be achieved by the coupling between matrix and particles that are responsive to various stimuli.

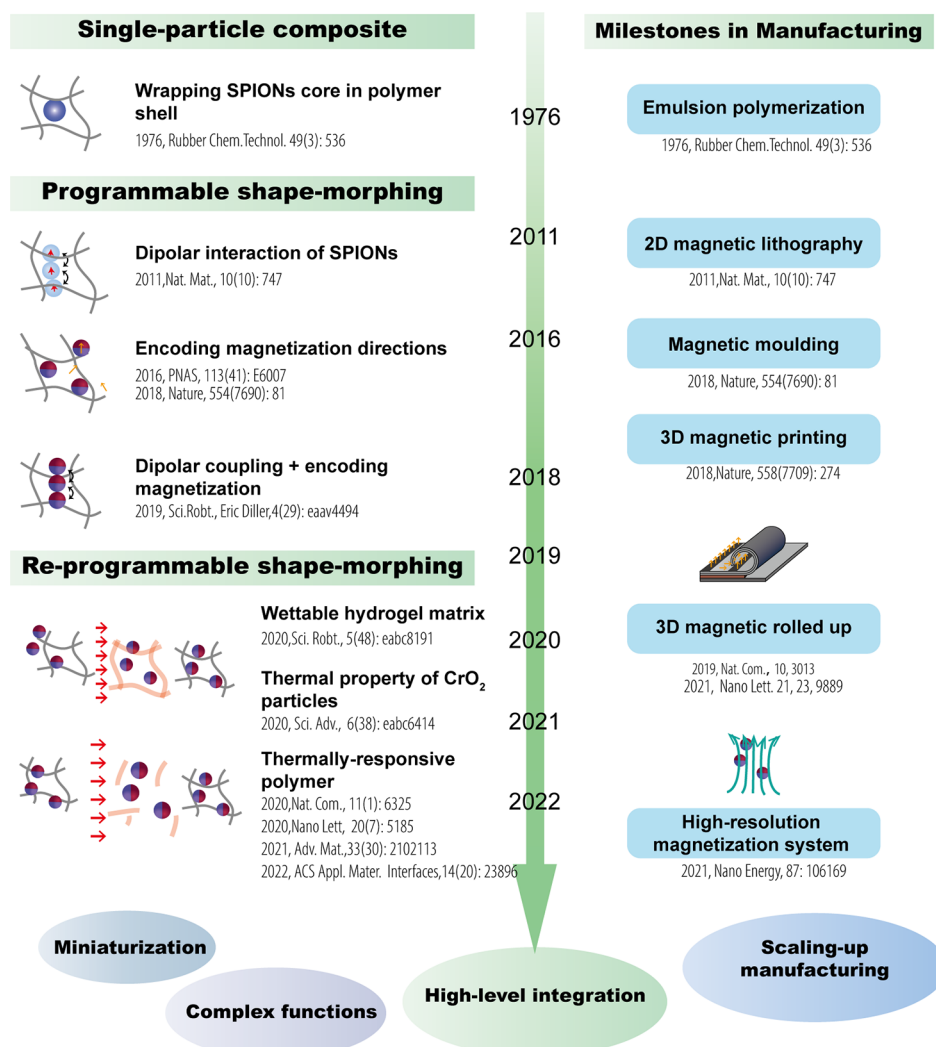


Figure 2. Technological roadmap depicting the trend of designing responsive magnetic composite nanostructures for smart microrobots. SPIONs: superparamagnetic iron oxide nanoparticles. Milestone achievements in manufacturing approaches and material design strategies for polymer–particle composites are highlighted in bold red texts and bold black texts, respectively.

Several review articles have been published in the field over the past decade focusing on promising biomedical applications,<sup>40</sup> material engineering,<sup>41–44</sup> bioinspired mechanisms,<sup>45</sup> multifunctionalities,<sup>46</sup> actuation mechanisms,<sup>7</sup> and systems.<sup>47</sup> Specifically, Wu et al. provided insights on multifunctional magnetic soft composites based on material design and structure fabrication.<sup>48</sup> Very recently, Kim and Zhao et al. provided a comprehensive design guideline for the optimal actuation performance of magnetic soft materials and robots.<sup>41</sup> Vijayasri K. et al. summarized the fabrication of magnetic polymer nanocomposites and their broad application spectrum in the biomedical field.<sup>40</sup> Our review is specifically focused on the micro- and nanofabrication technologies and design strategies for magnetic microrobots. Note that the scale of microrobots requires shrinking the size of a system while retaining high functionalities, which poses significant challenges to the manufacturing approaches and requires a more in-depth examination of the material–structure properties. On the basis of the features of magnetic shape-morphing microrobots, we highlight the niche applications enabled by magnetic microrobots. Additionally, we further compare the advantages and disadvantages of various fabrication methods

for microrobots and discuss promising manufacturing and material choices to adapt these robots to different application scenarios.

A direct comparison of different power sources for microrobots is further shown in Table 1. It is noteworthy that the development of magnetically powered polymer–particle composite structures is of utmost significance in the field, as magnetic fields possess the ability to penetrate tissues with ease and are widely utilized in clinical applications, such as magnetic resonance imaging. The precise control of microrobots using magnetic fields, coupled with various imaging modalities for feedback, is a key advantage. Additionally, magnetic fields allow for the reconfiguration of robots in diverse ways, unlike other stimuli, such as light, temperature, or chemicals, which may pose risks to certain biological materials. A great advantage of such systems is that biological environments are typically devoid of magnetism, which enables the deployment of these devices for sensing and actuation without background interference. Furthermore, magnetically powered microrobots exhibit the ability to virtually access any part of the body, in contrast to chemical/biohybrid robots that are constrained to specific organs. Similarly, ultrasound-based

robots can also be maneuvered remotely, but their controllability is limited because acoustic waves have primarily been employed for propulsion.

## TECHNOLOGICAL TREND OF DESIGNING AND MANUFACTURING RESPONSIVE MAGNETIC COMPOSITE STRUCTURES

Here, we outlined a technological roadmap showing the development of smaller, softer, and smarter systems from polymer–particle magnetic nanocomposites (Figure 2). The versatility of programming magnetic states in various types of magnetic particles embedded in polymer matrices offers a high degree of freedom in designing magnetically controlled microscale devices.

The field of microrobotics is advancing rapidly, which is driven by progress in microfabrication and nanofabrication techniques, including wet-chemistry-based emulsion polymerization, top-down photolithography, and bottom-up 3D printing. Besides, researchers are innovatively exploiting the properties of magnetic particles and polymer matrix. A landmark event in the field was the production of uniform polymer–magnetic particle nanocomposites by emulsion polymerization, first demonstrated in 1976 when magnetic nanoparticles were introduced into a porous polystyrene polymer matrix to generate uniform-sized magnetic beads.<sup>15,58</sup> With the approach, magnetic nanoparticles were randomly distributed in the beads, and they were primarily applied for bioanalytical research as biomolecular carriers. The polystyrene magnetic beads represented an early form of “mobile microscale systems”, as they used external power sources to propel the entire structure in a tetherless manner. Integration of the application of active responsive particles with polymers made rapid advancements in the bioanalytical industry and biomedical research. The advances ultimately contributed to a common goal of developing a practical medical microrobotic device that could meet biological and biomedical needs. For instance, the polymeric surfaces of microcarriers were studied extensively for their specific targeting of cells and drug biomolecules, which has become a major capability for the modern concept of “medical microrobots.”

Despite advancements in wet-chemistry-based fabrication approaches, they are limited in controlling complex structures other than basic forms of spheres or rods.<sup>59,60</sup> Therefore, researchers have successfully engineered materials to allow more complex morphologies, e.g., needles,<sup>32</sup> helices,<sup>33</sup> and grippers.<sup>34</sup> Various material engineering capabilities have facilitated multiple locomotion modes and high degrees of freedom for system control. Innovations have been made to improve existing techniques, such as allowing programming magnetic anisotropy in soft polymer matrices, which has promoted the concept of “programmable magnetic micro-machines”. The concept was demonstrated by aligning superparamagnetic particles in polymer matrices with magnetic fields.<sup>61</sup> Such demonstration through photolithography benefited from progress in multidisciplinary approaches, as the technique was extensively used in the semiconductor industry to process computer chips. Following this, Sitti et al. devised similar strategies of programming 3D magnetic profiles of a composite structure filled with neodymium–iron–boron (NdFeB) particles,<sup>62,63</sup> which possessed strong remanent magnetization for information coding. The resultant devices had more locomotion modes and transduced stronger

magnetic forces and torques compared with their superparamagnetic counterparts. Advanced fabrication techniques, such as injection molding and high-resolution 3D printing, were applied in this field in recent years, which has enabled the manufacturing of highly complex and miniaturized micro-machines.<sup>64,65</sup> To obtain numerous reconfigurable shape-morphing modes in a single structure, magnetic robots with repeatedly programmed magnetic anisotropy were developed in 2020.<sup>66–69</sup>

Beyond conventional magnetic properties, researchers have explored a rich spectrum of unconventional magnetic properties previously investigated in the fundamental magnetics research communities. Some of the unconventional properties included the transition of magnetism at Curie temperature<sup>70</sup> and size-dependent coercivity of magnetic particles.<sup>71</sup> Recent developments have used different types of magnetic particles [e.g., Fe<sub>3</sub>O<sub>4</sub> particles as heaters under high-frequency magnetic field agitation and chromium dioxide (CrO<sub>2</sub>) particles as reprogrammable units]. These particles have been integrated into a single robotic body to enable reprogrammable magnetization of the structures.<sup>72</sup> Through the magneto-thermal effect, impressive remote-field reprogrammable capability has been realized. Besides the study of unconventional material properties, theoretical modeling and computational simulation are vital for designing the mechanical properties for desired shape morphing modes. One example of such an approach is the evolutionary design strategy proposed by Zhao et al., which integrates theoretical modeling and a genetic algorithm to calculate the deflections of a magnetic continuum device with specific magnetization and rigidity patterns under uniform magnetic fields.<sup>36,73,74</sup> These achievements highlight the power of leveraging multidisciplinary expertise in this field of research and development.

As guided by the roadmap, both responsive particles and polymer matrices play a vital role.<sup>67,75,76</sup> The former is special because the magnetization states of particles, including the direction and switching fields, can be encoded in their structure, composition, and spatial distributions. The encoded magnetic properties can be translated into forces and torques in the soft matrix materials, which is similar to programming the ensemble structures, to allow their use in the development of intelligent microrobots. Regarding this, a few classifications of the responsive particles and polymer matrices are highlighted, and how they interact with each other to achieve complex shape morphing features are discussed in the subsequent sections. In the following discussion of the key design strategies for translating polymer–magnetic particle composites into functional systems, we envision that these strategies could be generalized to develop multistimuli-controlled complex systems, thereby providing more possibilities for advanced microrobotics and biomedical applications.

## DESIGNING MAGNETIC RESPONSIVE POLYMER–PARTICLE NANOCOMPOSITES

Choosing the polymer matrix or substrates with appropriate stimuli-responsive properties and their coupling with the active particles embedded in them is strategically important for microrobotic designs, as the shape-morphing of polymer matrices can be attributed to the specific response to certain physical or chemical stimuli. The principle was demonstrated by a few pioneering designs of active particles and shapeable alloys and polymers into soft robots, which are described below. Understanding the underlying shape-morphing mech-

**Table 2.** Tunable Mechanical Properties of Soft Matrixes and Substrates

	functional materials	strategy for tunable mechanical properties	stiffness strength	references
PDMS substrate	PDMS with PDMS- <i>b</i> -PEO	UV exposure with photomask	~0.04 MPa and ~2.6 MPa	Gandla et al. <sup>87</sup>
	pure PDMS	curing temperature and time	800 kPa to ~10 MPa	Seghir et al. <sup>88</sup>
	PDMS/iron oxide magnetic nanoparticle composites	magnetic nanoparticle doping	150–450 kPa	Lussier et al. <sup>89</sup>
	pure PDMS	changing the ratio of precursors	0.75–1.65 MPa (ratio of part A and B, 12:1–6:1; 60 min curing time; 85 °C)	Hocheng et al. <sup>90</sup>
hydrogel	alginate	changing the volume of agent ( $\text{CaCl}_2$ ) and cross-linking time light-triggered calcium release from liposomes	39.8–273.35 kPa ~2 kPa to over 20 kPa	Naghieh et al. <sup>91</sup>
	alginate/PAAm	changing the cross-linkers ( $\text{Ca}$ and $\text{Fe}^{3+}$ ) of hydrogel in different areas	$\text{Fe}^{3+}$ cross-linked area: 330 kPa $\text{Ca}^{2+}$ cross-linked area: 40 kPa	Liu et al. <sup>93</sup>
	GelMA	• reversible control of stiffness using DNA cross-linkers • cross-linker removal via toehold-mediated strand displacement • cross-linker restoring by adding fresh dsDNA	500–1000 Pa	Buchberger et al. <sup>94</sup>
	PAAm	reversible stiffness control by carbonyl iron alignment under magnetic fields	• 0.1–0.14 kPa at 0 T • 60–90 kPa at 0.75 T	Abdeen et al. <sup>95</sup>
	PAAm	changing acrylamide and bis(acrylamide) concentrations	0.5–40 kPa	Díaz-Bello et al. <sup>96</sup>
low-melting point alloys	Cerrolow 117	solid/liquid phase change through Joule heating	~3 GPa for the solid state solid/liquid state: 40 MPa/1.5 MPa solid/liquid state: 0.86 GPa/95.2 kPa	Nelson et al. <sup>82,81</sup> Shintake et al. <sup>97</sup> Shan et al. <sup>98,99</sup>
	Galinstan alloy			
	gallium with Fe-microsized particles	alignment of magnetic particles in liquid metal	5–2000 kPa	Ren et al. <sup>100</sup>
shape memory polymer	thermoplastic polyurethane	phase changing through Joule heating	2–0.1 GPa	Floreano et al. <sup>101</sup>
	gallium@ polyurethane (Ga@PU) sponge	phase changing by heating	35–2008.9 kPa	Wu et al. <sup>102</sup>

anism of representative matrices with diverse stimuli-responsive characteristics is, thus, crucial. Additionally, researchers in this field continuously search for materials that can facilitate high-resolution structuring for system miniaturization.

**Selection of the Polymer Matrix.** The matrix forms a substrate in which particles are embedded, and it is an important component for designing intelligent microrobots (Figure 2). PDMS and hydrogels are used as common matrix materials as they have mechanical properties that can be tuned by changing the ratio of precursors, initiators, curing temperature, and UV exposure time (Table 2). Additionally, the tunable mechanical properties of the soft matrix increase the degree of freedom for shape-morphing by external stimuli. A single material matrix cannot meet all needs. When selecting the matrix, it is important to differentiate their properties from target applications for microrobot design.

**Hydrogels.** Hydrogels are biphasic, porous, and water-permeable materials and include a big family of pH-responsive, anionic, and thermally responsive hydrogels. Hydrogels are highly promising matrix materials for medical microrobotic design and they have been widely studied for cell culture and *in vivo* delivery. They may respond to various stimuli, such as pH and ionic or temperature changes in the surrounding environment, and exhibit the shape-morphing ability of hydrogels by swelling or shrinking.<sup>77</sup> Although their degradable properties are favorable for removing the device from the body,

careful assessment is recommended after accounting for their retention time.

The alginate hydrogel matrix shrinks and swells in response to changes in the pH or ionic strength (e.g.,  $\text{Ca}^{2+}$ ). A class of ionic shape-morphing microrobotic end effectors can be constructed by loading alginate hydrogels with  $\text{CaCO}_3$  particles, which can couple with alginate through  $\text{H}^+$  ions.<sup>77</sup> In this design, water electrolysis generates  $\text{H}^+$  ions and leads to a rapid decrease in the pH. The ions then react with  $\text{CaCO}_3$  particles to generate  $\text{CO}_2$  and  $\text{Ca}^{2+}$  ions, which further react with sodium alginate to produce Ca-alginate gelation.

Similarly, microrobots of different morphologies can be fabricated with photosensitive hydrogels by selectively exposing the hydrogels to light. The available precursors for such types of robotic construction might include functional acrylic acids, the cross-linker dipentaerythritol pentaacrylate, and photoinitiators.<sup>78</sup> High pH values (e.g.,  $\text{pH} > 9$ ) deprotonate the carboxyl groups to generate electrostatic repulsive forces between molecular chains. The repulsion between molecular chains then results in the rapid swelling of the hydrogel network. When the carboxyl groups are protonated at low pH (e.g.,  $\text{pH} < 9$ ), the hydrogel network collapses and shrinks.

Hydrogels responsive to pH might be used in situations that require the sensing of certain physiological states of biofluids (e.g., gastric acid at  $\text{pH} = \sim 1.5$ ). However, the hydrogel matrix materials can only be used under certain circumstances because the uncontrollable *on/off* state of actuation must be

overcome. Additionally, they might face limitations during applications where high-speed actuation is required because of the slow response rates.

The use of thermally responsive hydrogels as a matrix allows the hydrogels to be coupled with the particles exhibiting photothermal or magnetothermal effects. The coupling between particles and the matrix allows programming the deformability of the ensemble structure through the patterning of the spatial distribution of particles. Poly(*N*-isopropylacrylamide) (PNIPAAm), with phase transition temperatures around 32–35 °C, is an extensively studied hydrogel matrix because of its low critical solution temperature, but unpolymerized residues remaining after PNIPAAm polymerization might cause neurotoxicity.<sup>79</sup> Alternatives, such as poly(ethylene glycol) and poly(3-caprolactone), might provide a wider selection. Representative photothermal particles include Au, for which its properties can be tuned by the shape and size of the particles. By patterning Au nanoparticles inside a thermal-responsive hydrogel (e.g., PDEAM hydrogel disk), a nonuniform temperature profile can be established through illumination under white light.<sup>80</sup> Thermally induced shape morphing might be advantageous for *in vivo* applications where body heat might be used to restore the shape of structures. However, this method has a few limitations, such as tissue damage caused by external light-induced heat. The light-induced heating for morphing the shape might not work inside the human body. In this respect, NIR-absorbing particles should be assessed as active particles for thermal coupling.<sup>3</sup>

**Nonconventional Soft Matrix Materials.** Nonconventional soft matrix materials have gained popularity. Among them, low-melting-point alloys and shape-memory polymers provide ideas for designing biocompatible medical robots. Although low-melting-point alloys have not been directly examined using magnetic microrobotic systems, a catheter made of a low-melting-point alloy with variable stiffness sheds some light on their potential.<sup>81,82</sup> Such alloys have a melting temperature slightly above the body temperature (47 °C) and are stable in the air. Below the melting temperature, they are a solid characterized by a Young's modulus of 3 GPa and tensile strength on the order of tens of MPa. The stiffness can be modulated through heating.<sup>83</sup> Above the melting temperature, the catheter segments become soft, and the mechanical performance is similar to that of a silicone tube.

In shape-memory polymers (SMPs), such as DiAPLEX MM5520, the stiffness can be tuned by varying the temperature above the glass transition temperature by applying an external stimulus, such as photothermal or Joule heating.<sup>84</sup> The property allows a structure to be reconfigured photothermally and magnetically, for example, by compositing magnetic iron microparticles and the shape-memory polymer (DiAPLEX MM5520). Under illumination, the composite structure softens and can respond to the excitation of an external magnetic field. Magnetic robots operating on the basis of this principle can pick up and release objects repeatedly by light and magnetic field stimulation. Tracy et al. proposed magnetic soft robots on the basis of iron microparticles with an average diameter of 4.2 μm in the DiAPLEX MM5520.<sup>85</sup> They also demonstrated reconfigurable magnetic origami actuators on the basis of the composite of magnetic NdFeB micro-particles dispersed in a shape-memory polymer matrix (DiAPLEX MM5520).<sup>86</sup> These ultrathin actuators can accomplish sequential folding and recovery with hinge locations programmed on the fly.

**Selection of Magnetic Functional Particles.** The shape-morphing ability of a composite structure encapsulating magnetic particles was achieved by the mechanical transduction from magnetic particles to the soft polymer matrix or through transmitting heat from magnetic particles to thermoresponsive polymers, such as hydrogels, using an alternating magnetic field or laser to excite the magnetic particles.<sup>63</sup> Recent advancements have shown the capability of the above mechanisms. For example, Wang et al. obtained shape-morphing magnetic PNIPAm hydrogels stimulated by an alternating magnetic field.<sup>29</sup> The temperature of the magnetic gels could increase from 20.5 to 38.0 °C within 240 s. The actuation speed could be further modulated by adding magnetic microparticles with strong magnetization (5 μm NdFeB particles).

The property of a magnetic particle can be described by its magnetization curve, expressed by

$$\vec{M} = \chi \vec{H}$$

Here,  $\chi$  indicates magnetic susceptibility. Depending on the value of  $\chi$ , the magnetic microparticles and nanoparticles can be paramagnetic ( $\chi > 0$ ) or ferromagnetic ( $\chi \gg 0$ ). For a magnetic robot with homogeneous magnetization created from magnetic particles and nonmagnetic polymer matrices, its magnetization ( $\vec{M}$ ) is proportional to the external magnetic field ( $\vec{H}$ ):  $\vec{M} = \chi \vec{H}$ , where  $\chi$  is constant. However, for a magnetic robot with nonhomogeneous magnetization,  $\chi$  becomes a tensor and is determined by the spatial distribution of its magnetic particles and the magnetization orientation of magnetic particles. This provides opportunities to configure the magneto-mechanical properties of the final structure on demand, thereby modifying the compressive or tensile stress of the structure for shape-morphing.

Stress in a magnetic composite structure can originate from two types of magnetic forces.<sup>7,41</sup> First, a magnetic particle in a magnetic field tries to align with the external magnetic field. The torque ( $\vec{\tau}$ ) is determined by the magnetic moment of the building block ( $\vec{m}$ ) and the magnetic flux density ( $\vec{B}$ ):  $\vec{\tau} = \vec{m} \times \vec{B}$ . Second, a magnetic functional building block can feel a translational force ( $\vec{F}$ ) toward the highest flux density when exposed to a magnetic field gradient:  $F_x = \nabla(\vec{m} \times \vec{B})$ . The magnetic force exerted on the magnetic particles can be further passed onto a soft material matrix, thereby leading to the deformation of the ensemble structure. In such cases, the simulation and subsequent substantiation of different magnetic configurations in a material matrix enable the programmable shape-morphing ability of a structure. With magnetic forces/torques, various shape-morphing modes have been realized, which include bending,<sup>61,103</sup> stretching/compressing,<sup>104</sup> and twisting.<sup>105</sup> With a time-varying magnetic field, programmable shape morphing can further lead to multiple locomotion modes, such as crawling,<sup>61</sup> rolling,<sup>67</sup> and walking (Figure 2).<sup>63</sup>

The main types of active magnetic particles used for constructing microrobots (Figure 2) with different properties, according to their corresponding dimensions and composition, include superparamagnetic nanoparticles (<50 nm),<sup>61,105</sup> single-domain nanomagnets (100–500 nm),<sup>71,106</sup> multidomain microscale (1–10 μm),<sup>36,70,107</sup> and milliscale (>1 mm) ferromagnets.<sup>108,109</sup>

**Superparamagnetic Nanoparticles (<50 nm).** Assemblies of superparamagnetic nanoparticles possess no remanence when magnetic hysteresis is measured at typical experimental time scales relevant for quasi-static measurements and can be

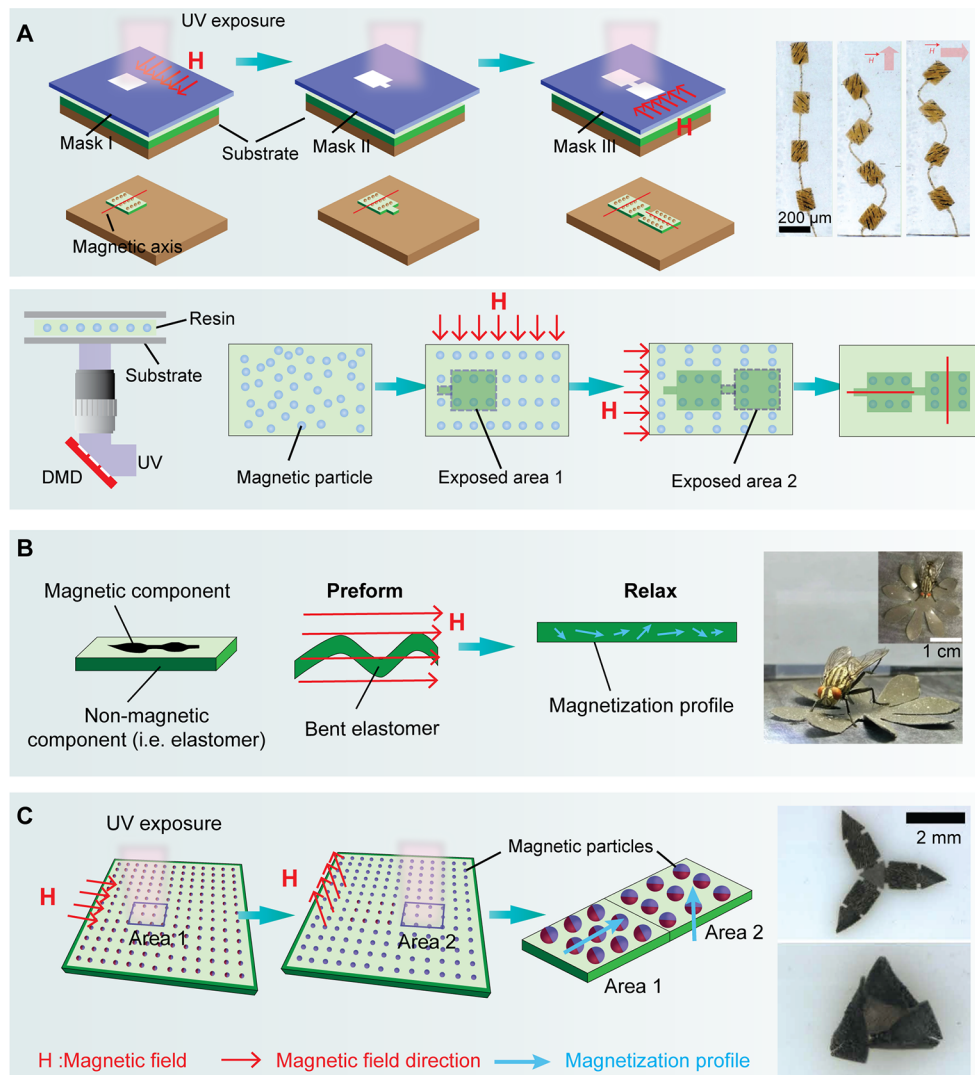


**Figure 3.** Representative approaches to fabricating microstructures of single shape-morphing modes. (A) Real-time (re)aligning magnetic nanoparticles combined with selective curing using mask-based (top panel) or DMD-based (bottom panel) lithography.<sup>61</sup> The magnetic nanoparticles mixed in the photocurable resin aligned into nanochains under a magnetic field applied in one direction. Then, photolithography was performed to define the shape of the microstructure. A magnetic field was applied in another direction, followed by the same lithography process to form an integral microstructure with a different magnetic axis. (Right panel) A microactuator containing four different easy axes recoils. (B) Magnetizing permanent magnet microparticles in a bending soft elastomer exposed to a uniform magnetic field.<sup>62</sup> The programming of the magnetic soft elastomer consisted of two components, including a magnetic component with NdFeB particles and a nonmagnetic component with aluminum (Al) powder. The desired orientation profile of magnetization was created by bending the soft elastomer when applied to a strong magnetization field. The magnitude profile of magnetization was produced by the width of the magnetic component. (Right panel) A flower-shaped magnetic soft-bodied robot catching a living fly.<sup>113</sup> (C) Reorienting permanentized magnetic particles within the selected UV curing regions.<sup>65</sup> Permanentized magnetic particles were reoriented under the controlled magnetic field, and UV curing froze the magnetic particles within the selected area. (Right panel) Magnetic triarm structures with programmed magnetization profiles.

randomly dispersed in a polymer matrix in the absence of a magnetic field.<sup>103</sup> They can be aligned to form nanochains in a magnetic field by minimizing the dipole interaction energy. The chains can be realigned by changing the direction of the external magnetic field. This property of superparamagnetic nanoparticles can lead to a versatile approach to programming anisotropy in a polymeric matrix.<sup>61,105</sup> A photosensitive polymer matrix, such as PEG-DA, after light exposure can freeze the anisotropy direction after the nanoparticle chains are formed. On the basis of this property, various types of smart polymeric actuators and microrobots have been made.<sup>61,105</sup>

**Single-Domain Nanomagnets (100–500 nm).** Single-domain nanomagnets are characterized by stable remanent magnetization.<sup>71</sup> They are suitable for designing microrobots with encoded magnetization directions. The strength of the external magnetic field needed for switching the direction of magnetization is called “coercivity,” which is influenced by the size and surface effect of the nanomagnets.<sup>110</sup> For example, the magnetic switching field of a stadium-shaped nanomagnet, which consists of a rectangle with one semicircle at each end with the width of the rectangle matching the diameter of the semicircle, can be engineered by modulating its aspect ratio ( $l/d$ , where  $l$  indicates the length,  $d$  indicates the width) at the

same volume  $V_0$  and the same thickness  $t_0$ .<sup>106</sup> The coercivity of a nanomagnet increases with the aspect ratio ( $C_r = l/d = d + \frac{\frac{V_0}{t_0} - \pi(0.5d)^2}{d}$ ), and decreases drastically with the decrease in the particle size until upon the transition to the superparamagnetic limit reaches zero. Single-domain magnets may possess uniaxial anisotropy. The anisotropy energy of a single domain particle with uniaxial anisotropy depends on the particle size:  $E = K_1 V_0 \sin \theta^2$ , where  $K_1$  indicates the anisotropy constant,  $V_0$  indicates the particle volume, and  $\theta$  indicates the angle between the easy axis and the magnetization vector.

**Permanent Magnetic Microparticles.** Permanent magnetic microparticles (e.g., 5 μm NdFeB microparticles typically possess a coercive field of ~690 mT) require a strong magnetic field for magnetization (typically a uniform field of several T is needed).<sup>111,112</sup> Permanent microparticles dispersed into a prepolymer can be reoriented by an external magnetic field locally.<sup>65</sup> Using this method, the magnetization profile of the permanent magnets in the polymer matrix can be programmed.

**Milliscale Magnets.** Milliscale magnets (e.g., NdFeB magnets) show stable dipole moments for the construction of similar or even larger scale systems.<sup>81,108,109</sup> Unlike the typical way of using a magnetic field to line up magnetic microparticles or nanoparticles, the dipolar interactions between the milliscale magnets are hard to modulate because magnetic dipoles tend to form simple chainlike or ringlike structures to minimize magnetic energy. This issue was addressed by Nelson et al., who proposed a magnetic quadrupole module composed of two permanent magnets inside a 3D-printed square case.<sup>108</sup> Two magnets can be arbitrarily arranged with a relative angle between their dipole moments. Each module has a dominant quadrupole moment and a small dipole moment that can govern the near-field interactions with neighboring modules and encode magnetization, respectively.

## MANUFACTURING: BASIC SINGLE-MODE SHAPE-MORPHING STRUCTURES

**Magnetic-Field-Assisted Lithography Patterning with Superparamagnetic Particles.** This technique was initially reported by Kwon et al. (Figure 3A).<sup>61</sup> It involves the alignment of superparamagnetic nanoparticles (e.g., 120 nm Fe<sub>3</sub>O<sub>4</sub> colloids) in a polymer matrix using a magnetic field, followed by the solidification of the polymer to freeze the chains of superparamagnetic nanoparticles. The magnetic axis of the nanochains of superparamagnetic nanoparticles can be fixed in multiple polymerized regions. UV-curable materials, such as PEG-DA, are used to prepare the magnetic premixes, which are then pipetted into a mold, including a microfluidic channel<sup>114</sup> or a glass mound constructed using coverslip spacers.<sup>3</sup> Magnetic nanoparticles can freely move in the UV-curable liquid resin. Once polymerized, the UV-curable resin becomes solid and further fixes the aligned nanoparticles. The shape of a microstructure is defined by photomasks<sup>3</sup> or a digital micromirror device (DMD) modulator.<sup>61</sup> The process can be repeated multiple times for different magnetic field directions to realign the superparamagnetic nanoparticles along different field lines in multiple parts. The nanochains in the polymer result in magnetic anisotropy and induce torque for shape morphing. Magnetic-field-assisted photolithography allows a lateral resolution of ~2 μm<sup>61</sup> and patterning with multiple exposures, but this method is limited to 2D

microstructures. Bionic microrobots (e.g., polymeric microlooper and flagellated microrobots) and scalable microrobots were fabricated by this method to achieve bioinspired locomotion,<sup>61</sup> adaptive locomotion,<sup>103</sup> color-barcoded micro-particles,<sup>114</sup> and biosensors.<sup>3</sup>

**Preformed Elastomers with Embedded Permanent Magnets (e.g., NdFeB Microparticles<sup>62–65</sup> and NdPrFeB<sup>107</sup>).** The method involves programming the magnetization profile of permanent magnetic microparticles in a preformed soft elastomer body (Figure 3B).<sup>62</sup> The soft elastomer is generally constructed from an active component of permanent magnetic microparticles and a passive component of nonmagnetic particles. Permanent magnetic particles embedded in the polymer matrix can be magnetized using a strong field (>1 T). The magnetization of the particles in the elastomers generates the magnetic torque to deform the robots. The shape-morphing modes depend on the magnetization profile of the soft robots.

Predeforming the elastomer can preset the orientation of the embedded magnetic particles. Using this method, the magnetization profile of the magnetic particles in the soft elastomer can be defined by bending the elastomer in a magnetic field, and the magnitude of the magnetization profile can be evaluated on the basis of the width of the magnetic component. To achieve the desired shape morphing, the continuum magnetization profile  $m(s)$  along the body of the robot, the required magnetic field  $B(t)$ , and the spatial field gradient of  $B(t)$  can be computed by optimizing Fourier coefficients<sup>62</sup> in which  $s$  is the desired deformations along the beam's length, and  $t$  is the time. With an optimized  $m(s)$ , the magnetization magnitude can be confirmed by adjusting the width of the magnetic component, and the orientation profile of magnetization can be obtained by using jigs to deform the elastomer beam in the magnetic field. On the basis of this method, multimodal locomotion (e.g., rolling, walking, and jumping) can be achieved with a time-varying magnetic field.<sup>63</sup> Additionally, dynamic maneuverability can be achieved, including active steering and navigation, for minimally invasive surgery.<sup>36,73</sup> The dimension of microrobots achieved in previous studies was ~1 cm<sup>62</sup> and 3.7 mm,<sup>63</sup> which was because relatively large molds were used for preforming the body of the microrobot. Wang et al. proposed ultrafast soft-bodied robots on the basis of NdFeB microparticles and the PDMS substrate.<sup>113</sup> A thin magnetic film (about 7 μm) was generated by spin coating, and a ready-to-use magnetic soft robot was obtained by high-throughput engraving or cutting of the magnetic film. These robots performed large-degree deformations at high frequencies of up to 100 Hz, which were driven at very low magnetic fields down to 0.5 mT and exhibited a high specific energy density of 10.8 kJ m<sup>-3</sup> mT<sup>-1</sup>.

**Direct Laser Curing of Permanent Magnets.** This technique was initially used by Diller et al. (Figure 3C).<sup>65</sup> In this technique, the magnetic particles are immobilized in the selected area of a polymer matrix using a laser beam. A magnetic field is used to set the direction of magnetization of the magnetic particles during the laser-induced polymerization process. A strong magnetic field of ~1 T is needed for magnetizing the particles. A stepper motor equipped with a permanent magnet is used to generate the required field strength and direction. This method shares similarities with magnetic-field-assisted lithography patterning by utilizing superparamagnetic particles. In this approach, premagnetized particles are uniformly mixed in UV-curable materials, and

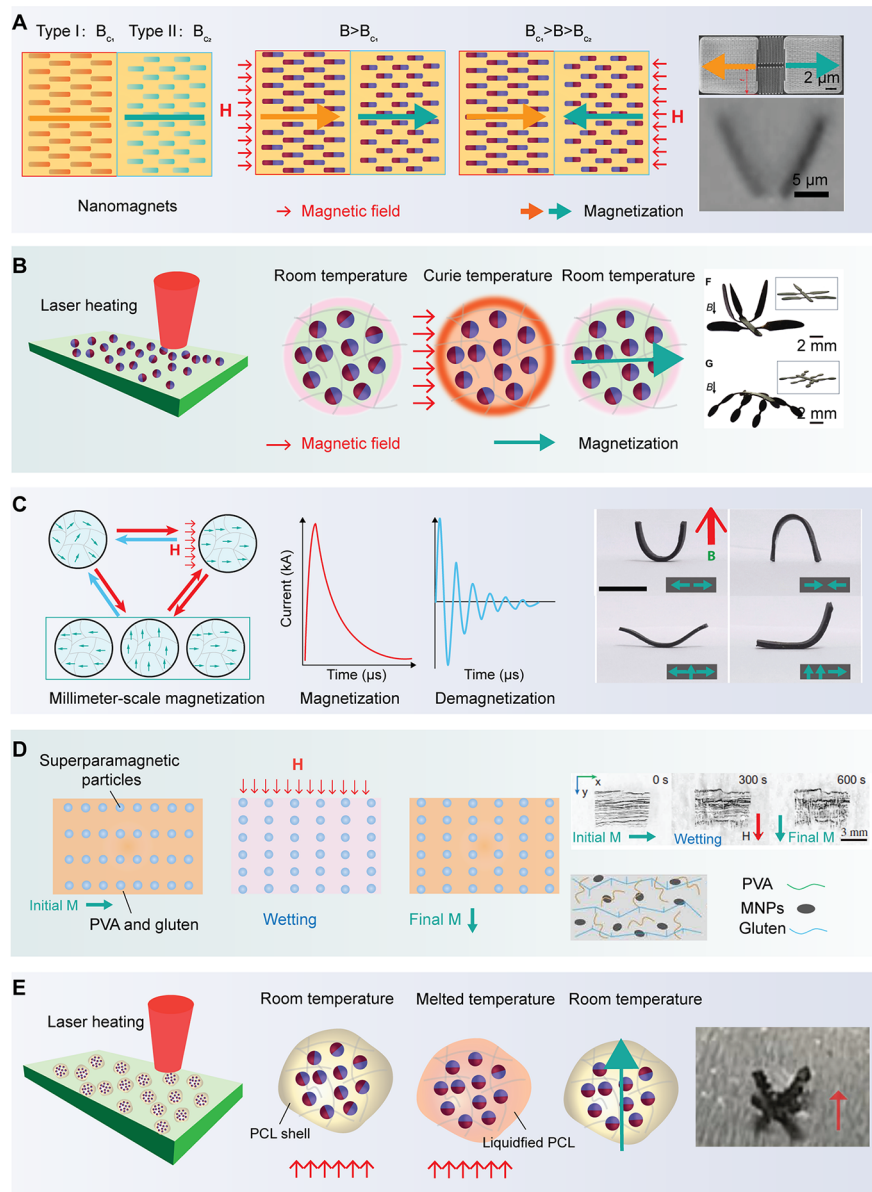


**Figure 4.** Reprogrammable magnetic configuration. (A) Encoding the magnetization of nanomagnet arrays with different magnetic switching fields.<sup>71</sup> Two types of single-domain nanomagnet arrays possess different coercive fields,  $B_{c1}$  and  $B_{c2}$  ( $B_{c1} > B_{c2}$ ). By applying a magnetic field  $B_1 > B_{c1}$ , both type I and type II nanomagnets are magnetized. Then, a lower magnetic field,  $B_{c2} < B_2 < B_{c1}$ , is applied in the opposite direction to remagnetize type II nanomagnets. The right panel is the resultant shape morphing. (B) Heat-assisted reprogrammable configurations by heating ferromagnetic particles above the Curie temperature.<sup>70,115</sup> The chromium dioxide ( $\text{CrO}_2$ ) ferromagnetic microparticles ( $\sim 10 \mu\text{m}$ , Curie temperature of  $118^\circ\text{C}$ ) are encapsulated in polydimethylsiloxane (PDMS) elastomer. A NIR laser generates the local heating effect. When the temperature is higher than the Curie temperature, the particles are demagnetized and lose the remanent magnetization. The magnetization profile can be redefined by applying a desired magnetic field during the cooling process by shutting down the laser. The right panel is the resultant shape morphing through the programmed magnetic profile in the robot body. (C) Reconfigurable magnetization process on the basis of high-resolution magnetization system.<sup>67</sup> A dual-coil magnetization system is set up with millisecond magnetization resolution. The permanent magnetic particles are randomly dispersed in the polymer matrix. Both oscillating and nonoscillating pulsed fields are used for magnetizing and demagnetizing, respectively. The required magnetic field directions are realized by modulating the current flow direction, which can define the orientation profile in the sample area. The right panel is the reprogrammed magnetization profile. (D) Swelling-assisted reprogrammable configurations by wetting the hydrogel.<sup>68</sup> Iron particles are encapsulated by PVA hydrogel and gluten. The easy magnetization axis is realized by aligning the magnetic particles along the external magnetic field. After wetting the hydrogel material, the easy magnetization axis can be reprogrammed by a magnetic field of  $200 \text{ mT}$ . (E) Reprogramming the magnetic anisotropy by laser on the basis of a meltable magnetic nanocomposite. Permanent NdFeB microparticles are encapsulated in the phase-changing polymer, polycaprolactone (PCL), to form the NdFeB@PCL microparticles.<sup>66</sup> The NdFeB@PCL microparticles are further encapsulated into the silicone matrix to fabricate the magnetic responsive soft material. Magnetic microparticles can absorb photon energy from the laser and melt the surrounding PCL polymer. The resolution of patterning is determined by a laser writing system ( $\text{CO}_2$  laser). The NdFeB@PCL microparticles are randomly oriented in the film. During the heating process, the magnetic microparticles in the PCL shell are realigned. The PCL shell possesses a lower melting temperature than the silicone matrix, which allows low energy to heat the PCL shell with minimal damage to the silicone. The realigned microparticle can be frozen in the PCL after removing the laser.

subsequently, multilayer 3D morphologies with programmable 3D magnetization profiles are fabricated through layer-by-layer laser curing.

Bionic microrobots, such as a multilegged structure or a multiarm magnetic microgripper, can be fabricated using the above approach with defined morphologies and magnetic profiles for bioinspired locomotion or cargo delivery. This method can be used to encode the magnetic particles in planar materials with arbitrary 3D orientation and a geometrical feature size of 100  $\mu\text{m}$ . Typical laser-curing printing can achieve a feature size of several micrometers, but the theoretical feature size in this magnetic patterning method was limited by the size of the permanent magnetic particles (e.g., 5  $\mu\text{m}$  NdFeB).

### EMERGING STRATEGIES: RECONFIGURABLE AND MULTIMODAL SHAPE-MORPHING MICROROBOTS

There is a certain degree of freedom for reconfiguring the magnetization profile before or after the fabrication of a micromachine body, but none of the strategies can reprogram the magnetization profile *in situ* once the particles are fixed in the magnetic soft composite. Consequently, very limited shape-morphing modes for soft microrobots were achieved using the previous approaches. In this section, we summarized the emerging strategies that were developed to reconfigure the magnetization profile of a structure, which were based on leveraging the differential physical properties of magnetic particles, including coercivity, Curie temperature, and the melting points of polymer matrices. We also discussed the crucial aspects of high-resolution magnetization systems for the development of reconfigurable microrobots (Figure 4).

**Magnetic Switching Fields of Particles.** For the same volume, the switching field of a nanomagnet (e.g., ferromagnetic objects) increases with its aspect ratio ( $l/d$ ) (Figure 4A).<sup>71</sup> On the basis of this property, two panel arrays of nanomagnets of different aspect ratios were constructed with reconfigurable shape-morphing modes [Figure 4A, where Panel I has a higher coercive field ( $B_{c1}$ ) than Panel II ( $B_{c2}$ )]. In this setup, when a magnetic field  $B_1$  ( $B_1 > B_{c1}$ ) is applied, nanomagnet arrays in the two panels are saturated along the field direction. Then, at a lower magnetization field  $B_2$  ( $B_{c2} < B_2 < B_{c1}$ ) applied in the opposite direction, the magnetization of nanomagnets with lower coercivity can be switched in the direction of the field. Alternatively, nanomagnets magnetized in two opposite directions can be achieved by the same approach to total  $2^2 = 4$  magnetic configurations for this two-panel device. Nanomagnet arrays can generate magnetic torques under an external magnetic field. A zigzag hinge spring between the rigid nanomagnet arrays facilitates the shape morphing. This method based on nanofabrication technology has great potential in the scalability of microrobots, ranging from submicrometric panels with a single nanomagnet up to millimeter-sized devices. Additionally, the switching time of each nanomagnet is in the range of a few nanoseconds, which is conducive to the rapid *in situ* reprogramming using a short (nanosecond to millisecond) magnetic field pulse.

**Curie Temperature.** Curie temperature is the temperature at which there is a magnetic phase transition from a ferromagnetic to a paramagnetic state. (Figure 4B).<sup>70,115</sup> Heating a permanent microparticle above its Curie temperature can facilitate the reorientation of the magnetic moment by applying low magnetic fields during cooling. As an example, CrO<sub>2</sub> microparticles are known to possess a relatively low

Curie temperature of 118 °C compared with other permanent magnetic materials. Above the Curie temperature, CrO<sub>2</sub> microparticles exhibit paramagnetic behavior. One common approach to heat these microparticles above the Curie temperature is the use of near-infrared (NIR) laser heating. Additionally, NIR heating offers a spatial resolution of approximately 40  $\mu\text{m}$ , which makes it suitable for precise localized heating in biomedical and bioengineering applications.

In addition, the magnetization reprogramming only requires a relatively low magnetization field (e.g., 15 mT). Furthermore, most soft elastomers are stable below the Curie temperature. For example, PDMS, which is thermally stable above 150 °C, allows the embedding of particles in a nanocomposite by thermal curing of the mixture of magnetic particles and PDMS. This remote programming on the basis of laser heating allows the adaptive operation of soft microrobots in confined and closed dynamic environments. However, the high heating temperature is unsuitable for biomedical applications, as it might cause thermal damage. Additionally, the laser-based reprogrammable method has limited penetration depth, which restricts its application in 3D magnetic structures.

**High-Resolution Magnetizing System.** A magnetizing system with a high spatial resolution allows direct rewriting of the magnetization profile in the operation area of a magnetic soft material (Figure 4C). Li et al. constructed a magnetizing system on the basis of two coils. This system has a pair of field shapers that can concentrate a pulsed magnetic field in a millimeter-scale region.<sup>67</sup> The field shaper consists of a flat cylinder made of CuCrZr alloy with a small cylinder on the upper surface, a hole at the center, and a slit along the radial direction. The flow of current is controlled by a crowbar circuit composed of a resistor, a diode, and a paralleled capacitor. Oscillating and nonoscillating currents can be generated by connecting and disconnecting the crowbar circuit with the coils. The two types of currents can be used for magnetization and demagnetization. A large amount of energy stored in the capacitor can result in a pulsed coil current and a rapidly changing magnetic field (0–2 T in the radial direction and 0–4 T in the axial direction in less than 1 ms) during the discharge process. This magnetic field induces an eddy current on the lower surface of the field shaper. Through the slit, the eddy current concentrates the pulsed magnetic field in the magnetization area. Compared with other reconfigurable magnetization methods, the magnetization resolution along the radial and axial directions are relatively low at about 7.6 and 4.6 mm, respectively. However, the magnetizing system can simplify the magnetization process. For example, the magnetization profile of a six-arm robot can be achieved in only one step. This method can be used to develop functional robots including, but not limited to, grippers, bionic robots, and wearable flexible actuators.

**Swelling Properties of Polymer Matrices.** By absorbing water, the spacing among magnetic particles in hydrogels can increase because of the swelling of the hydrogel, and the constraints to magnetic particles from hydrogels can greatly decrease (Figure 4D). When exposed to a magnetic field, the magnetic particles can be realigned along the field direction. Yang et al. developed millirobots on the basis of an agglutinate magnetic spray consisting of poly(vinyl alcohol) (PVA), gluten, and iron particles.<sup>68</sup> The magnetic spray can adhere to the surface of various objects as driving components. The iron particles are aligned along the external magnetic field and

fixed through thermal curing. PVA is known for its stability in still water because of its low solubility. The thermal curing process can effectively reduce the water content in PVA hydrogels, thereby leading to the fixation of magnetic particles within the hydrogel matrix. Furthermore, the constraints imposed by the magnetic particles in hydrogels can be modulated by altering the water content, which provides a means to finely tune the mechanical properties of the resulting composite materials.

After thermal curing, a thin and solidified magnetic film is obtained, named magnetic skin (M-skin). The easy magnetization axis of the M-skin is initially aligned and fixed along the horizontal direction. The easy magnetization axis can be turned  $90^\circ$  in 10 min under a 200 mT magnetic field under wetting. The millirobots can be actuated under a 50 mT magnetic field, which is lower than the strength for easy magnetization axis reprogramming (200 mT). Therefore, the millirobots coated with a magnetic spray can remain stable and locomote effectively in a fluid environment. Additionally, the magnetic spray is biocompatible with the host because it can be disintegrated.

**Melting Points of Polymer Matrices.** Melting the polymer matrix allows the magnetization profile of particles encapsulated in the polymer matrix to be modified.<sup>69</sup> A phase-change polymer, such as polycaprolactone (PCL), has a relatively lower melting temperature ( $>60^\circ\text{C}$ ) (Figure 4E). Recently, magnetic microparticles (e.g., 5  $\mu\text{m}$  NdFeB microparticles) were encapsulated in the PCL shell to prepare NdFeB@PCL microparticles.<sup>66</sup> The other polymer matrix with higher melting temperatures, such as a silicone matrix with thermal stability below 232  $^\circ\text{C}$ , was used to further encapsulate the NdFeB@PCL microparticles. Using two kinds of polymers with different melting points, the magnetization orientation can be reprogrammed by modulating the magnetic field at a medium temperature ( $>60^\circ\text{C}$ ). The silicone matrix is thermally stable below its melting point. After removing the laser from the selected area, the programmed magnetic orientations can be frozen again. With the reversible phase change of the PCL shell, the magnetic configuration can be reprogrammed by coordinating the laser scanning and the magnetic field control. On the basis of this method, reconfigurable soft robots and multistate electrical switches were produced.<sup>66</sup> Because a laser heating system is the most important part of the technique (e.g., CO<sub>2</sub> laser), the spatial resolution ( $\sim 300\ \mu\text{m}$ ) is limited by the laser spot size and particle size. The ultimate resolution is determined by the particle size.

## NICHE APPLICATIONS OF MAGNETIC SHAPE-MORPHING MICROROBOTS

The reconfigurable and multimodal shape-morphing micro-robots have the potential to offer biomedical applications as they are capable of adapting to complex and varying environments within the body, including cargo delivery,<sup>63</sup> minimally invasive surgery,<sup>36,112</sup> and sensing.<sup>116,117</sup>

**Cargo Delivery.** Shape-morphing microrobots, such as those with C-shape and gripper configurations, can effectively carry out cargo gripping and delivery by utilizing a required magnetic field.<sup>63</sup> For instance, Sitti et al. have developed strip-shaped small-scale robots that are able to locomote on tissue surfaces and pick up millimeter-scale cargo (measuring 1 mm  $\times$  0.8 mm  $\times$  1.5 mm) by curing into a C-shape. The cargo is then transported by rolling and maintaining the C-shape

configuration of the robot. During the transportation process, these microrobots may encounter various complex and hierarchical environments, such as wrinkles and cavities in the stomach. By utilizing rotating or gradient fields, the shape-morphing robots are capable of rolling or jumping in diverse locomotion environments. Once the desired position is achieved, the microrobots can release the cargo by uncurling. It is worth noting that these types of robots are typically utilized for transporting larger cargo, ranging from hundreds of microns to millimeters in size.

**Minimally Invasive Surgery.** Magnetic soft robots possess desirable traits for applications in minimally invasive surgery (MIS) because of their capabilities for remote control and deep-tissue penetration. The ability of magnetic soft robots to adapt their shape under high shear forces allows them to navigate through vessels that are significantly smaller than their diameter. The locomotion of microrobots in fluid-filled channels, such as blood vessels with changing physical and chemical conditions, represents a challenging task. Various functions of magnetic soft robots for use in MIS have been proposed, including shape adaptation of helical robots and omnidirectional steering of continuum robots.

Huang et al. proposed soft helical microswimmers that can continuously morph in response to the properties of the surrounding fluid.<sup>103</sup> These soft helical structures were fabricated by folding magnetic strips, and when a robot with a helix structure (with three turns, a radius of 1.25 mm, and a contour length of 33.3 mm) passed through a narrow channel ( $\sim 0.75\ \text{mm}$ ), it performed shape adaptation through the coordination between elastic and viscous stresses. The helical microrobots were able to recover their shape after passing through the narrow channel or corners because of their elastic deformation. Also, flexible ceramic-based thin films on the basis of magnetoelectric composites have been reported by Kim et al., thereby exhibiting reversible tunable magnetoelectric capabilities depending on the undergoing mechanical stretching.<sup>118</sup>

Small-scale magnetic continuum robots demonstrate the ability to actively steer and navigate in complex and constrained environments, such as blood vessels and lungs.<sup>36</sup> These soft continuum robots rely on programmed shape morphing, which grants them omnidirectional steering and navigating capabilities. The ferromagnetic composite used in these robots comprises unmagnetized ferromagnetic microparticles, such as NdFeB, embedded in soft materials like PDMS or thermoplastic polyurethane (TPU). The active magnetic end of these robots possesses an axial magnetization direction (M) that can be manipulated by the external magnetic field (B) generated by a permanent magnet. This allows the active magnetic tip to choose its path through the magnetic torque generated by the magnetic field. The performance of these magnetic robots is influenced by factors, such as particle concentration and aspect ratio, that impact their actuation abilities. In addition to their steering and navigating capabilities, these microscale continuum robots can be designed to incorporate additional functionalities. These functionalities may include steering fluidic transport,<sup>116</sup> steering laser delivery,<sup>36</sup> contact force generation,<sup>74</sup> reconfigurable shapes,<sup>119</sup> and real-time force monitoring,<sup>120</sup> thereby expanding their potential applications. It is worth noting that to optimize the workspace and achieve various reconfigurable shape-changing modes, there is a need for microscale

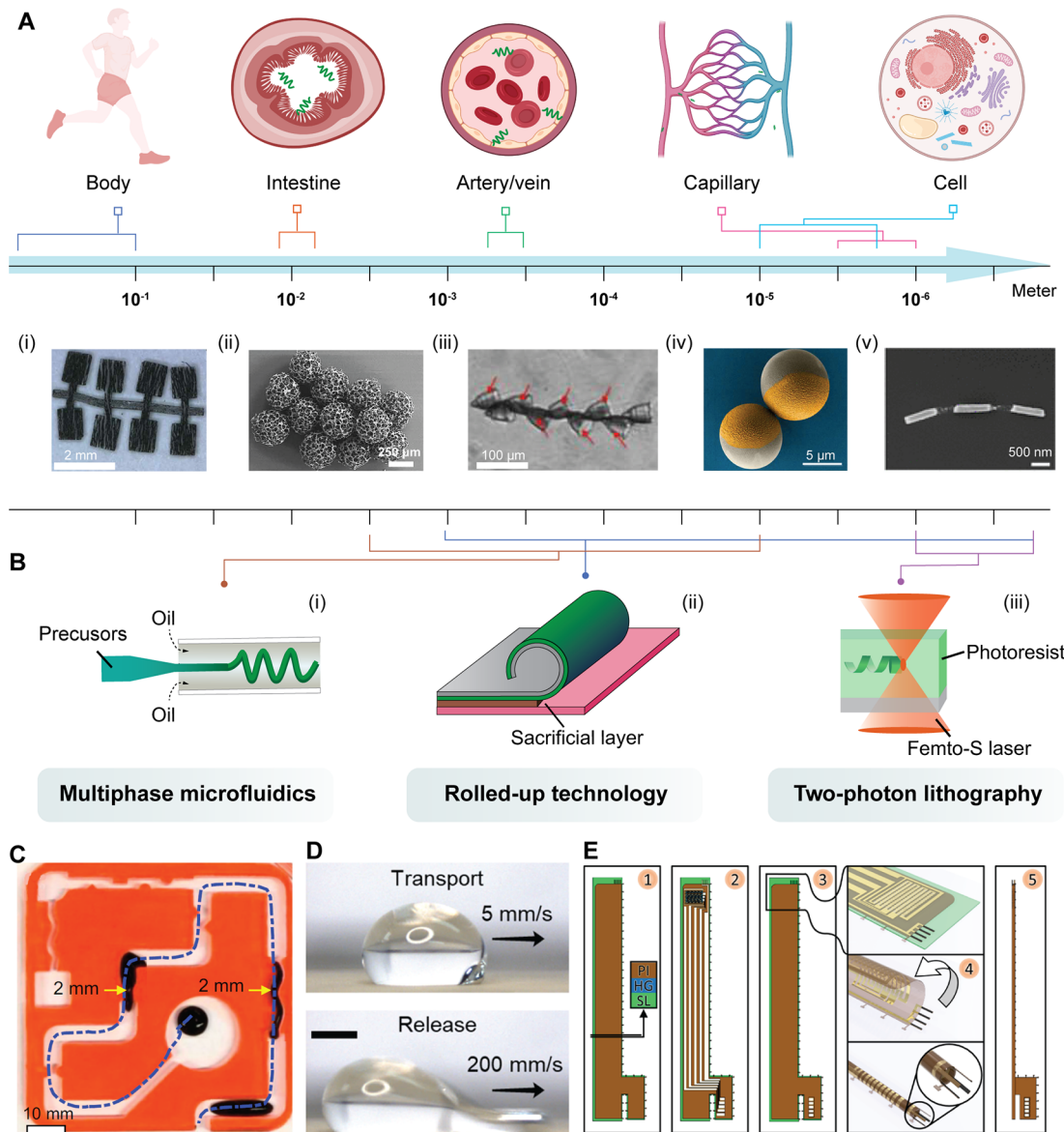


**Figure 5.** Promising manufacturing and material choices of next generation soft robots with multifunctionality and scalability. (A) Different types of robots with sizes ranging from milliscale to nanoscale compared with various human biological features, as presented on the top. (i) Milliscale multilegged robot locomotion capability in a milliscale channel (cross-section of the channel: 4.7 by 1.0 mm).<sup>65</sup> (ii) Spherelike microrobots (>100  $\mu\text{m}$ ) for knee cartilage regeneration *invivo*.<sup>59</sup> (iii) Sperm micromotors with a horned cap for drug delivery in venules (30 to 100  $\mu\text{m}$  in diameter).<sup>131</sup> (iv) Microrollers (~3.0 and ~7.8  $\mu\text{m}$  diameters) for drug delivery in postcapillary venules and veins (5–10  $\mu\text{m}$  diameter).<sup>132</sup> (v) Nanoscale magnetic swimmer for biomedical operation at the nanoscale.<sup>127</sup> (B) Advanced fabrication technology for small-scale robots. (i) Microfluidics emulsion technology is useful for microscopic robots ranging from several to hundreds of micrometers. (ii) Rolled-up technology is suitable for microscopic to nanoscale robots. (iii) Two-photon lithography possesses the highest resolution. (C–E) Softer robots, including ferrofluids,<sup>133</sup> magnetic liquid metal,<sup>134</sup> and self-assembling polymer films,<sup>116</sup> potentially negotiate through narrow and constrained spaces better than elastomer-based soft robots because of better deformability.

continuum robots with programmable magnetization and rigidity patterns.

**Sensing.** Environmental monitoring represents a significant application of magnetic soft robots. Sensing modules, such as magnetic sensors and fluorescence probes, can be integrated into magnetic shape-morphing robots to enable monitoring of the surrounding environments. Fluorescence imaging, which offers real-time and widefield imaging with high spatial resolution and is based on nonhazardous optical radiation and fluorescence labels, has shown promise in this regard. However, challenges remain, including the high light scattering

of live tissue, low signal-to-background ratio, and strong autofluorescence from live tissue.

In recent studies, *in vivo* imaging based on near-infrared (NIR) II light, including NIR-IIa (1300–1400 nm) and NIR-IIb (1500–1700 nm), has emerged as a potential solution to overcome these challenges.<sup>121–123</sup> NIR-II imaging offers microscale high-resolution imaging with subcentimeter penetration depth, low light scattering, and suppressed autofluorescence. For instance, microrobots incorporating lanthanide-doped nanocrystals have been used for detecting stomach acid. Among various actuation and sensing methods, the magnetic

**Table 3. Comparison of Different Methods to Fabricate Magnetic Soft Microrobots**

manufacturing methods	pros	cons	reference
microfluidics	- high throughput - functional material integration - good resolution (5–10 $\mu\text{m}$ ) - scalability	- limited morphologies, such as chainlike and helix	- Liu et al. <sup>157</sup> - Yoshida et al. <sup>126</sup>
roll-up technology	- 3D fabrication - on-board microelectronic circuits, engines, actuators, sensors, controllers, and power supplies, etc. - compatibility with semiconductor process - variable sizes from nanometer to micrometers	- limited material choices due to system requirements - fragility and reactive nature of 2D materials	- Xu et al. <sup>146</sup> - Bandari et al. <sup>117</sup> - Rivkin et al. <sup>116</sup>
photolithography	- submicrometer resolution (down to 180 nm) - compatibility with semiconductor process - high reproducibility	- high cost - 2D and simple 3D morphologies - requirement of clean room - requirement of a digital or physical mask - manual steps	- Miskin et al. <sup>135</sup> - Kim et al. <sup>61</sup>
molding	- simple process - scalability - good resolution (down to 300 $\mu\text{m}$ ) - compatibility with semiconductor process	- 2D (e.g., strip and rod) and simple 3D morphologies - requires a mold with cavities, such as glass tube or chip, fabricated by photolithography	- Hunter et al. <sup>158</sup> - Medina-Sánchez et al. <sup>159</sup>
3D printing	- 3D fabrication  - compatibility with semiconductor process - high reproducibility	- high cost for high-resolution fabrication  - challenges in biocompatibility - limited material choice - slow printing speed	- Dabbagh et al. <sup>160</sup> - Zhang et al. <sup>161</sup> - Xu et al. <sup>65</sup>

field is particularly advantageous because of its biocompatibility.

Rivkin et al. have made significant strides in integrating magnetic sensing components into the wall of magnetic continuum robots.<sup>116</sup> They have developed a flexible anisotropic magnetoresistive magnetic sensor that is sensitive to the external magnetic field aligned with the robot's long axis. This potential *in vivo* tracking technology offers exceptionally high tracking precision with submillimeter accuracy and reduces the need for invasive techniques, such as X-ray imaging for tracking purposes. The deformable magnetic sensor was transformed from a film into tubular devices using roll-up technology, thereby enabling seamless integration with the soft robot structure.

Furthermore, Bandari et al. have also successfully integrated radio frequency (RF) power supply into microscale soft robots to provide a potential self-powered stretchable sensing platform.<sup>117</sup> This innovative approach provides possibilities for using other power sources, such as biofluids (e.g., human sweat)<sup>124</sup> and human motion,<sup>125</sup> to drive stretchable sensors and wireless transmission modules on untethered magnetic soft robots.

In addition to embedding sensing modules, the monitoring of the change in the robotic shape emerged as a viable method for sensing in magnetic soft robots. Stimuli-responsive hydrogels, which can swell or shrink in response to surrounding stimuli, such as pH or temperature, have been utilized for this purpose. For instance, the helical shape of microrobots has been leveraged for propulsion, where a thermal-responsive hydrogel, such as p(NIPAM-*co*-AAC) and NaAlg, serves as the robotic body.<sup>126</sup> The helical shape can change in response to the surrounding fluidic environment and influence the mobility of the microrobots in terms of propulsion velocity and locomotion modes.

Li et al. proposed the use of magnetic nanocomposites with temperature-sensitive ferrites, such as CrO<sub>2</sub>, for shape change

monitoring.<sup>115</sup> Laser heating can reduce the magnetization of the magnetic nanocomposite, which results in an increase in the bending angle of a magnetic strip. The bending angle serves as a reflection of the magnetization of the magnetic nanocomposite. However, the identification of shape changes in microscale robots can be challenging because of the miniaturized features and potential interference from the surrounding environment.

Despite the direct reflection of changes in the surrounding environment through shape change, further research and development are needed to overcome the challenges associated with shape change monitoring in microscale robots.<sup>126</sup> The integration of stimuli-responsive hydrogels and magnetic nanocomposites into the design of magnetic soft robots offers promising opportunities for advancing the field of soft robotics and enabling sophisticated sensing capabilities.

## PERSPECTIVES ON PROMISING MANUFACTURING AND MATERIAL CHOICES

**Scalable Manufacturing Approaches.** Scalable manufacturing approaches are important for multifunctional micro-robots to interact with multiscale biological systems (Figure 5A; Table 3). Milliscale robots can work in relatively large organ cavities, such as the stomach and intestine.<sup>63,65</sup> Bio-hybrid microrobots, such as sperm micromotors, can move through small cavities (e.g., arteries, veins, and the oviduct channel).<sup>128–131</sup> Nanoscale robots are available for intracellular tasks. Several manufacturing methods have been developed to fabricate small-scale robots.<sup>127</sup> We predict that the rapid developments in MEMS/NEMS technologies, along with microfluidics, thin-film vacuum deposition techniques, and polymer-based strain engineering, can contribute to the fabrication of small biointerfacing devices with a higher degree of integration.<sup>135</sup>

**Multiphase Microfluidic Fabrication.** Multiphase microfluidic fabrication is a promising technique for producing

single/double emulsions and fiber structures because of its excellent control over fluid phases (Figure 5B).<sup>136,137</sup> Various microfluidic systems, including coaxially assembled capillary devices and 3D-printed and lithographically patterned microchannels, can produce monodispersed emulsions.<sup>138–140</sup> The method can be used to fabricate microscopic robots ranging from a few to several hundred micrometers and spherical or cylindrical morphologies, which are difficult to fabricate using other techniques.<sup>141–143</sup> More strategies might be developed with the technique to fabricate Janus-type or multicore–shell-type particles and fiber-shaped structures (e.g., micromotors) by adhering functional nanoparticles to microspheres functionalized with a photocurable polymer precursor. Moreover, because of the feasibility of encapsulating virtually any particle in the precursors, multiphase microfluidics fabrication allows a simple tailoring of physical and chemical responses of the fabricated structures under external stimuli (e.g., UV illumination, the concentration of H<sub>2</sub>O<sub>2</sub>, and the magnetic field). A technique to demonstrate magnetic robots on the basis of hierarchically assembled magnetic microparticles was developed recently. The layout of the cores could be adjusted from a linear-chain form to a triangular form.<sup>144,145</sup> Such robotic structures can perform large-scale locomotion, multiplexed DNA detection, and the facilitation of 3D imaging applications. This technique might help researchers in developing single-cell robotic carriers for bioengineering as it can be used to control cells and biomolecules at the microscopic scale with microfluidics. Additionally, the technique can be further developed to be equipped with magnetic field systems for more complex shape-morphing modes.

**Rolled-up Technology.** The rolled-up technology is powerful and can convert planar thin films (both organic and inorganic) into complex 3D fine structures.<sup>146</sup> It is scalable for the integration of thin-film-based components in single tubular microstructures and nanostructures.<sup>147</sup> Because the technology is compatible with semiconductor fabrication techniques, including thin-film deposition and etching, electronics-based sensors and signal transmitters might be integrated into the tubular structures. This is a promising strategy for the system-level realization of dust-scale microrobots. Recently, Schmidt et al. used a rolled-up technique to develop a flexible and motile twin-jet engine.<sup>117,148</sup> Electronic circuits were constructed in the platform for wireless energy transfer via inductive coupling. Fast and stable locomotion was achieved by using two microcatalytic engines with an optional heating wire integrated into a single microsystem. The approach provided a promising strategy for creating microsystems with monolithic integration of multifunctional components, such as circuits, electronic and optoelectronic devices, actuators, wireless power supplies, and wireless communication. On the basis of a derivative of rolled-up techniques, small electronic blood vessels (~2.3 mm) were produced by rolling up an MPC-PLC membrane into a tube,<sup>149</sup> which was applied for *in situ* electrical stimulation. This technology might enable on-chip power sources (e.g., batteries) to be integrated seamlessly into the system, though it is still challenging in the context of increased power density in a considerably smaller device.

**Three-Dimensional Laser Lithography.** Three-dimensional laser lithography<sup>10</sup> was applied to produce rocketlike micro-robots,<sup>39</sup> burrlike porous spherical microrobots,<sup>150</sup> and helical microcarriers.<sup>151,152</sup> For example, the two-photon polymerization lithography technique is an advanced approach based

on photocurable polymers, such as SU-8, IP-Dip, and IP-L. In this technique, a femtosecond laser and a direct patterning approach are used to produce 3D nanostructures. The minimum feature size of the 3D structures can reach 200 nm, and sub-100 nm resolution was achieved in 2D. High-resolution 3D fabrication techniques facilitate the development of submicrometer-scale robots. This technique promotes applications in intracellular sensing and fundamental mechanochemical research. The technology has been used to develop the smallest man-made jet engine and electronic blood vessels.<sup>52,149</sup> Complex objects can be produced using this fabrication method, such as spherical cages and helical architectures, which can be attached to polymeric chassis.<sup>153,154</sup> Nelson et al. developed a method of printing multimaterial architectures prepared as interlocked microstructures.<sup>153,154</sup> Moreover, this method can directly fabricate microstructures on various substrates, such optical coherence tomography endoscopy on a fiber tip<sup>155</sup> and fibroin hydrogel beam on a magnetic microparticle.<sup>156</sup> With this fabrication method, it became possible to realize three-dimensional metallic and polymeric components, like spherical cages or helical architectures, which can be threaded with polymeric chassis. This technology was used to produce a class of vehicles and robots in the millimeter and micrometer scale.

**Liquid and More Biocompatible Materials.** Materials-wise, liquid and more biocompatible materials, including ferrofluids,<sup>133</sup> magnetic liquid metal,<sup>134</sup> self-assembling polymer films,<sup>116</sup> and biotemplating,<sup>131,163</sup> may shift the paradigm of soft microrobot designs as these materials allow robots to pass through narrow and constrained spaces more effectively than elastomer-based soft robots because of better deformability (Figure 5C–E).

Ferrofluid droplets can adapt to confined spaces, such as smaller droplets in channels.<sup>133</sup> Compared with the soft helical structures based on magnetic nanocomposites, ferrofluid droplets are much softer and gentler. These ferrofluid droplets can be elongated and deformed to pass through confined spaces by programming the magnetic field. The ferrofluid droplets are naturally spherical because of surface tension, and a programmed magnetic field  $H$  can be applied using either electromagnets or permanent magnet arrays. The magnetic field induces shape morphing by exerting a magnetic force  $F(r) = -\nabla\mu_0(M \times H)$ , in which  $M$  is the magnetization [ $M = \chi(H_e + H_f(M))$ ],  $\mu_0$  is the magnetic permeability of the vacuum, and  $H$  consists of the applied magnetic field  $H_e$  and internally produced magnetic field  $H_f(M)$  to balance the surface tension  $F_s$ . Ferrofluid droplet robots possess both passive deformability from the external physical environment and active deformability from the external magnetic field. They can squeeze their body and pass through confined channels, and the minimum diameter of the channel they can pass through is influenced by the dynamic viscosity and volume of the ferrofluids, as well as the strength of the magnetic field. Additionally, ferrofluid robots have multiple functions, such as splitting and merging for cargo delivery or micromanipulation. Despite the challenges in doping functional materials, ferrofluid robots are expected to enable diverse and multiple functionalities for various applications, including critical lab-on-a-chip, bioengineering, and biomedical applications.

Magnetic liquid metals based on gallium (Ga) and Fe nanoparticles exhibit<sup>134</sup> fluidity-based adaptive deformability, which allows liquid metal robots (~1.25 mm in diameter) to manipulate droplets in challenging confined environments,

including via on-demand self-splitting, merging, and adaptive deformation in narrow channels. Although this technique is promising, further modifications need to be tested, such as engineering the interface of ferrofluids and liquid metals for attaching to molecules or targeting cells more efficiently. Multiphase microfluidic approaches might be further developed to encapsulate these liquids with a solid, such as an ultrasoft polymeric shell, using a special technique described above. Biohybrids might also be considered for developing soft robots.<sup>162</sup> The artificial components can be integrated into biological components, such as sperm cells,<sup>131,163</sup> *spirulina* microalgae,<sup>164</sup> and *Chlorella* cells.<sup>165</sup> Sperm-templated micro-robots might be developed on the basis of a single-step electrostatic self-assembly technique.<sup>163</sup> In a study, 100 nm iron oxide particles were attached to the surface of a bovine sperm cell, which enabled distributed actuation under an external magnetic field and maintained the flexibility of the microrobots. Such kinds of microrobots based on biotemplating have additional advantages, including adaptability to the physiological environment, facile cargo loading, and efficient motion at the microscale level.<sup>166</sup>

## AUTHOR INFORMATION

### Corresponding Authors

**Gungun Lin** – Institute for Biomedical Materials and Devices, School of Mathematical and Physical Sciences, Faculty of Science, University of Technology Sydney, Ultimo, NSW 2007, Australia;  [orcid.org/0000-0001-9880-8478](https://orcid.org/0000-0001-9880-8478); Email: [gungun.lin@uts.edu.au](mailto:gungun.lin@uts.edu.au)

**Mariana Medina-Sánchez** – Micro- and NanoBiomedical Engineering Group (MNBE), Institute for Integrative Nanosciences, Leibniz Institute for Solid State and Materials Research (IFW), 01069 Dresden, Germany; Chair of Micro- and NanoSystems, Center for Molecular Bioengineering (B-CUBE), Dresden University of Technology, 01062 Dresden, Germany; Email: [m.medina.sanchez@ifw-dresden.de](mailto:m.medina.sanchez@ifw-dresden.de)

**Dayong Jin** – Institute for Biomedical Materials and Devices, School of Mathematical and Physical Sciences, Faculty of Science, University of Technology Sydney, Ultimo, NSW 2007, Australia;  [orcid.org/0000-0003-1046-2666](https://orcid.org/0000-0003-1046-2666); Email: [dayong.jin@uts.edu.au](mailto:dayong.jin@uts.edu.au)

### Authors

**Yuan Liu** – Shenzhen Institute of Advanced Technology, Chinese Academy of Sciences, Shenzhen 518055 Guangdong Province, P. R. China

**Maria Guix** – Universitat de Barcelona, Departament de Ciència dels Materials i Química Física, Institut de Química Teòrica i Computacional Barcelona, 08028 Barcelona, Spain

**Denys Makarov** – Helmholtz-Zentrum Dresden-Rossendorf e.V., Institute of Ion Beam Physics and Materials Research, 01328 Dresden, Germany;  [orcid.org/0000-0002-7177-4308](https://orcid.org/0000-0002-7177-4308)

Complete contact information is available at:  
<https://pubs.acs.org/10.1021/acsnano.3c01609>

### Notes

The authors declare no competing financial interest.

## ACKNOWLEDGMENTS

The authors acknowledge the financial support from the Australian Research Council DECRA Fellowship (DE230100079, G.L.), the Australian Research Council

Industrial Transformational Research Hub for IDEAL (IH1S0100028, G.L. and D.J.), the National Natural Science Foundation of China (52203152, Y.L.), and the Shenzhen Outstanding Talents Training Fund (RCBS20221008093222008, Y.L.), Spanish Ministry of Science through the Ramon y Cajal Grant No. RYC2020-945030119-I (M.G.) and European Union's Horizon Europe Research and Innovation Programme under EVA project (GA No: 101047081, M.G.) and European Research Council (ERC) under the European Union's Horizon 2020 research and innovation program (grant agreement number: 853609, M.M.-S.).

## VOCABULARY

magnetic nanocomposites, engineered nanocomposites containing polymer matrix and magnetic materials; shape morphing, the process of forming something into a particular shape; reprogrammable magnetization, a mechanism of repatterning the magnetization profiles in the magnetic matter; scalable manufacturing, a method of fabricating small biointerfacing devices with a higher degree of integration; shape adaptation, the process of dynamically changing shapes to adapt to the surrounding environments

## REFERENCES

- (1) Nguyen, V. Du; Min, H. K.; Kim, H. Y.; Han, J.; Choi, Y. H.; Kim, C. S.; Park, J. O.; Choi, E. Primary Macrophage-Based Microrobots: An Effective Tumor Therapy in Vivo by Dual-Targeting Function and Near-Infrared-Triggered Drug Release. *ACS Nano* **2021**, *15*, 8492–8506.
- (2) Zhang, F.; Zhuang, J.; Li, Z.; Gong, H.; de Ávila, B. E. F.; Duan, Y.; Zhang, Q.; Zhou, J.; Yin, L.; Karshalev, E.; Gao, W.; Nizet, V.; Fang, R. H.; Zhang, L.; Wang, J. Nanoparticle-Modified Microrobots for in Vivo Antibiotic Delivery to Treat Acute Bacterial Pneumonia. *Nat. Mater.* **2022**, *21*, 1324–1332.
- (3) Liu, Y.; Lin, G.; Bao, G.; Guan, M.; Yang, L.; Liu, Y.; Wang, D.; Zhang, X.; Liao, J.; Fang, G.; Di, X.; Huang, G.; Zhou, J.; Cheng, Y.; Jin, D. Stratified Disk Microrobots with Dynamic Maneuverability and Proton-Activatable Luminescence for in Vivo Imaging. *ACS Nano* **2021**, *15*, 19924–19937.
- (4) Medina-Sánchez, M.; Schmidt, O. G. Medical microrobots need better imaging and control. *Nature* **2017**, *545*, 406.
- (5) Mujtaba, J.; Liu, J.; Dey, K. K.; Li, T.; Chakraborty, R.; Xu, K.; Makarov, D.; Barmin, R. A.; Gorin, D. A.; Tolstoy, V. P.; Huang, G.; Solovev, A. A.; Mei, Y. Micro-Bio-Chemo-Mechanical-Systems: Micromotors, Microfluidics, and Nanozymes for Biomedical Applications. *Adv. Mater.* **2021**, *33*, 2007465.
- (6) Wang, B.; Kostarelos, K.; Nelson, B. J.; Zhang, L. Trends in Micro-/Nanorobotics: Materials Development, Actuation, Localization, and System Integration for Biomedical Applications. *Adv. Mater.* **2021**, *33*, 2002047.
- (7) Zhou, H.; Mayorga-Martinez, C. C.; Pané, S.; Zhang, L.; Pumera, M. Magnetically Driven Micro and Nanorobots. *Chem. Rev.* **2021**, *121*, 4999–5041.
- (8) Schmidt, C. K.; Medina-Sánchez, M.; Edmondson, R. J.; Schmidt, O. G. Engineering Microrobots for Targeted Cancer Therapies from a Medical Perspective. *Nature Communications*. **2020**, *11*, 5618.
- (9) Aziz, A.; Pane, S.; Iacovacci, V.; Koukourakis, N.; Czarske, J.; Menciassi, A.; Medina-Sánchez, M.; Schmidt, O. G. Medical Imaging of Microrobots: Toward in Vivo Applications. *ACS Nano* **2020**, *14*, 10865–10893.
- (10) Rajabasadi, F.; Schwarz, L.; Medina-Sánchez, M.; Schmidt, O. G. 3D and 4D Lithography of Untethered Microrobots. *Progress in Materials Science*. **2021**, *120*, 100808.

- (11) Han, M.; Guo, X.; Chen, X.; Liang, C.; Zhao, H.; Zhang, Q.; Bai, W.; Zhang, F.; Wei, H.; Wu, C.; Cui, Q.; Yao, S.; Sun, B.; Yang, Y.; Yang, Q.; Ma, Y.; Xue, Z.; Kwak, J. W.; Jin, T.; Tu, Q.; Song, E.; Tian, Z.; Mei, Y.; Fang, D.; Zhang, H.; Huang, Y.; Zhang, Y.; Rogers, J. A. Submillimeter-Scale Multimaterial Terrestrial Robots. *Sci. Robot.* **2022**, *7*, abn0602.
- (12) Chen, Y.; Pan, R.; Wang, Y.; Guo, P.; Liu, X.; Ji, F.; Hu, J.; Yan, X.; Wang, G. P.; Zhang, L.; Sun, Y.; Ma, X. Carbon Helical Nanorobots Capable of Cell Membrane Penetration for Single Cell Targeted SERS Bio-Sensing and Photothermal Cancer Therapy. *Adv. Funct. Mater.* **2022**, *32*, 2200600.
- (13) Tawk, C.; Sariyildiz, E.; Alici, G. Force Control of a 3D Printed Soft Gripper with Built-In Pneumatic Touch Sensing Chambers. *Soft Robot.* **2022**, *9*, 970–980.
- (14) Zhang, Y.; Zhang, L.; Yang, L.; Vong, C. I.; Chan, K. F.; Wu, W. K. K.; Kwong, T. N. Y.; Lo, N. W. S.; Ip, M.; Wong, S. H.; Sung, J. J. Y.; Chiu, P. W. Y.; Zhang, L. Real-Time Tracking of Fluorescent Magnetic Spore-Based Microrobots for Remote Detection of C. Diff Toxins. *Sci. Adv.* **2019**, *5*, No. eaau9650.
- (15) Moerland, C. P.; Van IJzendoorn, L. J.; Prins, M. W. J. Rotating Magnetic Particles for Lab-on-Chip Applications-a Comprehensive Review. *Lab on a Chip.* **2019**, *19*, 919–933.
- (16) Kummer, M. P.; Abbott, J. J.; Kratochvil, B. E.; Borer, R.; Sengul, A.; Nelson, B. J. Octomag: An Electromagnetic System for 5-DOF Wireless Micromanipulation. *IEEE Trans. Robot.* **2010**, *26*, 1006–1017.
- (17) Van Oene, M. M.; Dickinson, L. E.; Pedaci, F.; Köber, M.; Dulin, D.; Lipfert, J.; Dekker, N. H. Biological Magnetometry: Torque on Superparamagnetic Beads in Magnetic Fields. *Phys. Rev. Lett.* **2015**, *114*, 218301.
- (18) Wang, Y.; Liu, X.; Chen, C.; Chen, Y.; Li, Y.; Ye, H.; Wang, B.; Chen, H.; Guo, J.; Ma, X. Magnetic Nanorobots as Maneuverable Immunoassay Probes for Automated and Efficient Enzyme Linked Immunosorbent Assay. *ACS Nano* **2022**, *16*, 180–191.
- (19) Hu, W.; Alici, G. Bioinspired Three-Dimensional-Printed Helical Soft Pneumatic Actuators and Their Characterization. *Soft Robot.* **2020**, *7*, 267–282.
- (20) Gao, C.; Wang, Y.; Ye, Z.; Lin, Z.; Ma, X.; He, Q. Biomedical Micro-/Nanomotors: From Overcoming Biological Barriers to In Vivo Imaging. *Adv. Mater.* **2021**, *33*, 2000512.
- (21) Guimarães, C. F.; Gasperini, L.; Marques, A. P.; Reis, R. L. The Stiffness of Living Tissues and Its Implications for Tissue Engineering. *Nature Reviews Materials.* **2020**, *5*, 351–370.
- (22) Iwaso, K.; Takashima, Y.; Harada, A. Fast Response Dry-Type Artificial Molecular Muscles with [C2]Daisy Chains. *Nat. Chem.* **2016**, *8*, 625–632.
- (23) Cheng, Y.; Chan, K. H.; Wang, X. Q.; Ding, T.; Li, T.; Lu, X.; Ho, G. W. Direct-Ink-Write 3D Printing of Hydrogels into Biomimetic Soft Robots. *ACS Nano* **2019**, *13*, 13176–13184.
- (24) Yu, C.; Duan, Z.; Yuan, P.; Li, Y.; Su, Y.; Zhang, X.; Pan, Y.; Dai, L. L.; Nuzzo, R. G.; Huang, Y.; Jiang, H.; Rogers, J. A. Electronically Programmable, Reversible Shape Change in Two- and Three-Dimensional Hydrogel Structures. *Adv. Mater.* **2013**, *25*, 1541–1546.
- (25) Fan, W.; Shan, C.; Guo, H.; Sang, J.; Wang, R.; Zheng, R.; Sui, K.; Nie, Z. Dual-Gradient Enabled Ultrafast Biomimetic Snapping of Hydrogel Materials. *Sci. Adv.* **2019**, *5*, No. eaav7174.
- (26) Han, D.; Farino, C.; Yang, C.; Scott, T.; Browe, D.; Choi, W.; Freeman, J. W.; Lee, H. Soft Robotic Manipulation and Locomotion with a 3D Printed Electroactive Hydrogel. *ACS Appl. Mater. Interfaces* **2018**, *10*, 17512–17518.
- (27) Xue, B.; Qin, M.; Wang, T.; Wu, J.; Luo, D.; Jiang, Q.; Li, Y.; Cao, Y.; Wang, W. Electrically Controllable Actuators Based on Supramolecular Peptide Hydrogels. *Adv. Funct. Mater.* **2016**, *26*, 9053–9062.
- (28) McCracken, J. M.; Rauzan, B. M.; Kjellman, J. C. E.; Su, H.; Rogers, S. A.; Nuzzo, R. G. Ionic Hydrogels with Biomimetic 4D-Printed Mechanical Gradients: Models for Soft-Bodied Aquatic Organisms. *Adv. Funct. Mater.* **2019**, *29*, 1806723.
- (29) Tang, J.; Yin, Q.; Qiao, Y.; Wang, T. Shape Morphing of Hydrogels in Alternating Magnetic Field. *ACS Appl. Mater. Interfaces* **2019**, *11*, 21194–21200.
- (30) Wang, X.; Feng, J.; Yu, H.; Jin, Y.; Davidson, A.; Li, Z.; Yin, Y. Anisotropically Shaped Magnetic/Plasmonic Nanocomposites for Information Encryption and Magnetic-Field-Direction Sensing. *Research* **2018**, *2018*, 7527825.
- (31) Li, Z.; Qian, C.; Xu, W.; Zhu, C.; Yin, Y. Coupling Morphological and Magnetic Anisotropy for Assembling Tetragonal Colloidal Crystals. *Sci. Adv.* **2021**, *7*, No. eabh1289.
- (32) Zhang, X.; Chen, G.; Fu, X.; Wang, Y.; Zhao, Y. Magneto-Responsive Microneedle Robots for Intestinal Macromolecule Delivery. *Adv. Mater.* **2021**, *33*, 2104932.
- (33) Schwarz, L.; Karnaushenko, D. D.; Hebenstreit, F.; Naumann, R.; Schmidt, O. G.; Medina-Sánchez, M. A Rotating Spiral Micromotor for Noninvasive Zygote Transfer. *Adv. Sci.* **2020**, *7*, 2000843.
- (34) Gouda, S. R.; Yasa, I. C.; Hu, X.; Ceylan, H.; Hu, W.; Sitti, M. Biodegradable Untethered Magnetic Hydrogel Milli-Grippers. *Adv. Funct. Mater.* **2020**, *30*, 2004975.
- (35) Yan, G.; Xu, B.; Shi, X.; Zong, Y.; Wu, Y.; Liu, J.; Ouyang, Y.; Chen, G.; Cui, J.; Mei, Y. Anisotropic Magnetized Tubular Microrobots for Bioinspired Adaptive Locomotion. *Appl. Mater. Today* **2022**, *27*, 101457.
- (36) Kim, Y.; Parada, G. A.; Liu, S.; Zhao, X. Ferromagnetic Soft Continuum Robots. *Sci. Robot.* **2019**, *4*, aax7329.
- (37) Li, J.; Singh, V. V.; Sattayasamitsathit, S.; Orozco, J.; Kaufmann, K.; Dong, R.; Gao, W.; Jurado-Sánchez, B.; Fedorak, Y.; Wang, J. Water-Driven Micromotors for Rapid Photocatalytic Degradation of Biological and Chemical Warfare Agents. *ACS Nano* **2014**, *8*, 11118–11125.
- (38) Dong, R.; Zhang, Q.; Gao, W.; Pei, A.; Ren, B. Highly Efficient Light-Driven TiO<sub>2</sub>-Au Janus Micromotors. *ACS Nano* **2016**, *10*, 839–844.
- (39) Li, D.; Liu, C.; Yang, Y.; Wang, L.; Shen, Y. Micro-Rocket Robot with All-Optic Actuating and Tracking in Blood. *Light Sci. Appl.* **2020**, *9*, 84.
- (40) K, V.; Tiwari, A. A Review on Magnetic Polymeric Nanocomposite Materials: Emerging Applications in Biomedical Field. *Inorganic and Nano-Metal Chemistry.* **2023**, *1*.
- (41) Kim, Y.; Zhao, X. Magnetic Soft Materials and Robots. *Chem. Rev.* **2022**, *122*, 5317–5364.
- (42) Kirillova, A.; Ionov, L. Shape-Changing Polymers for Biomedical Applications. *J. Mater. Chem. B* **2019**, *7*, 1597–1624.
- (43) Apsite, I.; Salehi, S.; Ionov, L. Materials for Smart Soft Actuator Systems. *Chem. Rev.* **2022**, *122*, 1349–1415.
- (44) Ning, X.; Wang, X.; Zhang, Y.; Yu, X.; Choi, D.; Zheng, N.; Kim, D. S.; Huang, Y.; Zhang, Y.; Rogers, J. A. Assembly of Advanced Materials into 3D Functional Structures by Methods Inspired by Origami and Kirigami: A Review. *Advanced Materials Interfaces.* **2018**, *5*, 1800284.
- (45) Palagi, S.; Fischer, P. Bioinspired Microrobots. *Nat. Rev. Mater.* **2018**, *3*, 113–124.
- (46) Yuk, H.; Wu, J.; Zhao, X. Hydrogel Interfaces for Merging Humans and Machines. *Nat. Rev. Mater.* **2022**, *7*, 935–952.
- (47) Yang, Z.; Zhang, L. Magnetic Actuation Systems for Miniature Robots: A Review. *Adv. Intell. Syst.* **2020**, *2*, 2000082.
- (48) Wu, S.; Hu, W.; Ze, Q.; Sitti, M.; Zhao, R. Multifunctional Magnetic Soft Composites: A Review. *Multifunct. Mater.* **2020**, *3*, 042003.
- (49) Sanchez, S.; Soler, L.; Katuri, J. Chemically Powered Micro- and Nanomotors. *Angew. Chemie - Int. Ed.* **2015**, *54* (5), 1414–1444.
- (50) Soler, L.; Magdanz, V.; Fomin, V. M.; Sanchez, S.; Schmidt, O. G. Self-Propelled Micromotors for Cleaning Polluted Water. *ACS Nano* **2013**, *7*, 9611–9620.
- (51) Sitti, M. Miniature Soft Robots - Road to the Clinic. *Nature Reviews Materials.* **2018**, *3*, 74–75.
- (52) Magdanz, V.; Guix, M.; Hebenstreit, F.; Schmidt, O. G. Dynamic Polymeric Microtubes for the Remote-Controlled Capture,

- Guidance, and Release of Sperm Cells. *Adv. Mater.* **2016**, *28*, 4084–4089.
- (53) Ji, Q.; Moughames, J.; Chen, X.; Fang, G.; Huaroto, J. J.; Laude, V.; Martínez, J. A. I.; Ulliac, G.; Clévy, C.; Lutz, P.; Rabenorosoa, K.; Guelpa, V.; Spangenberg, A.; Liang, J.; Mosset, A.; Kadlec, M. 4D Thermomechanical Metamaterials for Soft Microrobotics. *Commun. Mater.* **2021**, *2*, 93.
- (54) Aghakhani, A.; Yasa, O.; Wrede, P.; Sitti, M. Acoustically Powered Surface-Slipping Mobile Microrobots. *Proc. Natl. Acad. Sci. U. S. A.* **2020**, *117*, 3469–3477.
- (55) Ren, L.; Nama, N.; McNeill, J. M.; Soto, F.; Yan, Z.; Liu, W.; Wang, W.; Wang, J.; Mallouk, T. E. 3D Steerable, Acoustically Powered Microswimmers for Single-Particle Manipulation. *Sci. Adv.* **2019**, *5*, No. eaax3084.
- (56) Martella, D.; Nocentini, S.; Nuzhdin, D.; Parmeggiani, C.; Wiersma, D. S. Photonic Microhand with Autonomous Action. *Adv. Mater.* **2017**, *29*, 1704047.
- (57) Jing, W.; Chowdhury, S.; Guix, M.; Wang, J.; An, Z.; Johnson, B. V.; Cappelleri, D. J. A Microforce-Sensing Mobile Microrobot for Automated Micromanipulation Tasks. *IEEE Trans. Autom. Sci. Eng.* **2019**, *16*, 518–530.
- (58) Ugelstad, J.; Hansen, F. K. Kinetics and Mechanism of Emulsion Polymerization. *Rubber Chem. Technol.* **1976**, *49*, 536–609.
- (59) Go, G.; Jeong, S. G.; Yoo, A.; Han, J.; Kang, B.; Kim, S.; Nguyen, K. T.; Jin, Z.; Kim, C. S.; Seo, Y. R.; Kang, J. Y.; Na, J. Y.; Song, E. K.; Jeong, Y.; Seon, J. K.; Park, J. O.; Choi, E. Human Adipose-Derived Mesenchymal Stem Cell-Based Medical Microrobot System for Knee Cartilage Regeneration in Vivo. *Sci. Robot.* **2020**, *5*, aay6626.
- (60) Vyskocil, J.; Mayorga-Martinez, C. C.; Jablonská, E.; Novotný, F.; Ruml, T.; Pumera, M. Cancer Cells Microsurgery via Asymmetric Bent Surface Au/Ag/Ni Microrobotic Scalpels through a Transversal Rotating Magnetic Field. *ACS Nano* **2020**, *14*, 8247–8256.
- (61) Kim, J.; Chung, S. E.; Choi, S. E.; Lee, H.; Kim, J.; Kwon, S. Programming Magnetic Anisotropy in Polymeric Microactuators. *Nat. Mater.* **2011**, *10*, 747–752.
- (62) Lum, G. Z.; Ye, Z.; Dong, X.; Marvi, H.; Erin, O.; Hu, W.; Sitti, M. Shape-Programmable Magnetic Soft Matter. *Proc. Natl. Acad. Sci. U. S. A.* **2016**, *113*, E6007–E6015.
- (63) Hu, W.; Lum, G. Z.; Mastrangeli, M.; Sitti, M. Small-Scale Soft-Bodied Robot with Multimodal Locomotion. *Nature* **2018**, *554*, 81–85.
- (64) Kim, Y.; Yuk, H.; Zhao, R.; Chester, S. A.; Zhao, X. Printing Ferromagnetic Domains for Untethered Fast-Transforming Soft Materials. *Nature* **2018**, *558*, 274–279.
- (65) Xu, T.; Zhang, J.; Salehizadeh, M.; Onaizah, O.; Diller, E. Millimeter-Scale Flexible Robots with Programmable Three-Dimensional Magnetization and Motions. *Sci. Robot.* **2019**, *4*, No. eaav4494.
- (66) Deng, H.; Sattari, K.; Xie, Y.; Liao, P.; Yan, Z.; Lin, J. Laser Reprogramming Magnetic Anisotropy in Soft Composites for Reconfigurable 3D Shaping. *Nat. Commun.* **2020**, *11*, 6325.
- (67) Ju, Y.; Hu, R.; Xie, Y.; Yao, J.; Li, X.; Lv, Y.; Han, X.; Cao, Q.; Li, L. Reconfigurable Magnetic Soft Robots with Multimodal Locomotion. *Nano Energy* **2021**, *87*, 106169.
- (68) Yang, X.; Shang, W.; Lu, H.; Liu, Y.; Yang, L.; Tan, R.; Wu, X.; Shen, Y. An Agglutinate Magnetic Spray Transforms Inanimate Objects into Millirobots for Biomedical Applications. *Sci. Robot.* **2020**, *5*, abc8191.
- (69) Song, H.; Lee, H.; Lee, J.; Choe, J. K.; Lee, S.; Yi, J. Y.; Park, S.; Yoo, J. W.; Kwon, M. S.; Kim, J. Reprogrammable Ferromagnetic Domains for Reconfigurable Soft Magnetic Actuators. *Nano Lett.* **2020**, *20*, 5185–5192.
- (70) Alapan, Y.; Karacakol, A. C.; Guzelhan, S. N.; Isik, I.; Sitti, M. Reprogrammable Shape Morphing of Magnetic Soft Machines. *Sci. Adv.* **2020**, *6*, No. eabc6414.
- (71) Cui, J.; Huang, T. Y.; Luo, Z.; Testa, P.; Gu, H.; Chen, X. Z.; Nelson, B. J.; Heyderman, L. J. Nanomagnetic Encoding of Shape-Morphing Micromachines. *Nature* **2019**, *575*, 164–168.
- (72) Tang, J.; Sun, B. Reprogrammable Shape Transformation of Magnetic Soft Robots Enabled by Magnetothermal Effect. *Appl. Phys. Lett.* **2022**, *120*, 244101.
- (73) Wang, L.; Zheng, D.; Harker, P.; Patel, A. B.; Guo, C. F.; Zhao, X. Evolutionary Design of Magnetic Soft Continuum Robots. *Proc. Natl. Acad. Sci. U. S. A.* **2021**, *118*, e2021922118.
- (74) Wang, L.; Guo, C. F.; Zhao, X. Magnetic Soft Continuum Robots with Contact Forces. *Extrem. Mech. Lett.* **2022**, *51*, 101604.
- (75) Kuang, X.; Wu, S.; Ze, Q.; Yue, L.; Jin, Y.; Montgomery, S. M.; Yang, F.; Qi, H. J.; Zhao, R. Magnetic Dynamic Polymers for Modular Assembling and Reconfigurable Morphing Architectures. *Adv. Mater.* **2021**, *33*, 2102113.
- (76) Pozhitkova, A. V.; Kladko, D. V.; Vinnik, D. A.; Taskaev, S. V.; Vinogradov, V. V. Reprogrammable Soft Swimmers for Minimally Invasive Thrombus Extraction. *ACS Appl. Mater. Interfaces* **2022**, *14*, 23896–23908.
- (77) Zheng, Z.; Wang, H.; Dong, L.; Shi, Q.; Li, J.; Sun, T.; Huang, Q.; Fukuda, T. Ionic Shape-Morphing Microrobotic End-Effectors for Environmentally Adaptive Targeting, Releasing, and Sampling. *Nat. Commun.* **2021**, *12*, 411.
- (78) Xin, C.; Jin, D.; Hu, Y.; Yang, L.; Li, R.; Wang, L.; Ren, Z.; Wang, D.; Ji, S.; Hu, K.; Pan, D.; Wu, H.; Zhu, W.; Shen, Z.; Wang, Y.; Li, J.; Zhang, L.; Wu, D.; Chu, J. Environmentally Adaptive Shape-Morphing Microrobots for Localized Cancer Cell Treatment. *ACS Nano* **2021**, *15*, 18048–18059.
- (79) Lanzalaco, S.; Armelin, E. Poly(N-Isopropylacrylamide) and Copolymers: A Review on Recent Progresses in Biomedical Applications. *Gels.* **2017**, *3*, 36.
- (80) Kim, H.; Kang, J. H.; Zhou, Y.; Kuenstler, A. S.; Kim, Y.; Chen, C.; Emrick, T.; Hayward, R. C. Light-Driven Shape Morphing, Assembly, and Motion of Nanocomposite Gel Surfers. *Adv. Mater.* **2019**, *31*, 1900932.
- (81) Chautems, C.; Tonazzini, A.; Boehler, Q.; Jeong, S. H.; Floreano, D.; Nelson, B. J. Magnetic Continuum Device with Variable Stiffness for Minimally Invasive Surgery. *Adv. Intell. Syst.* **2020**, *2*, 1900086.
- (82) Lussi, J.; Mattmann, M.; Sevim, S.; Grigis, F.; De Marco, C.; Chautems, C.; Pané, S.; Puigmartí-Luis, J.; Boehler, Q.; Nelson, B. J. A Submillimeter Continuous Variable Stiffness Catheter for Compliance Control. *Adv. Sci.* **2021**, *8*, 2101290.
- (83) Hao, Y.; Gao, J.; Lv, Y.; Liu, J. Low Melting Point Alloys Enabled Stiffness Tunable Advanced Materials. *Adv. Funct. Mater.* **2022**, *32*, 2201942.
- (84) Aksoy, B.; Shea, H. Reconfigurable and Latchable Shape-Morphing Dielectric Elastomers Based on Local Stiffness Modulation. *Adv. Funct. Mater.* **2020**, *30*, 2001597.
- (85) Liu, J. A. C.; Gillen, J. H.; Mishra, S. R.; Evans, B. A.; Tracy, J. B. Photothermally and Magnetically Controlled Reconfiguration of Polymer Composites for Soft Robotics. *Sci. Adv.* **2019**, *5*, No. eaaw2897.
- (86) Ha, M.; Cañón Bermúdez, G. S.; Liu, J. A. C.; Oliveros Mata, E. S.; Evans, B. A.; Tracy, J. B.; Makarov, D. Reconfigurable Magnetic Origami Actuators with On-Board Sensing for Guided Assembly. *Adv. Mater.* **2021**, *33*, 2008751.
- (87) Gandla, S.; Gupta, H.; Pininti, A. R.; Tewari, A.; Gupta, D. Highly Elastic Polymer Substrates with Tunable Mechanical Properties for Stretchable Electronic Applications. *RSC Adv.* **2016**, *6*, 107793–107799.
- (88) Seghir, R.; Arscott, S. Extended PDMS Stiffness Range for Flexible Systems. *Sensors Actuators, A Phys.* **2015**, *230*, 33–39.
- (89) Lussier, R.; Giroux, Y.; Thibault, S.; Rodrigue, D.; Ritcey, A. M. Magnetic Soft Silicone Elastomers with Tunable Mechanical Properties for Magnetically Actuated Devices. *Polym. Adv. Technol.* **2020**, *31*, 1414–1425.
- (90) Hocheng, H.; Chen, C. M.; Chou, Y. C.; Lin, C. H. Study of Novel Electrical Routing and Integrated Packaging on Bio-Compatible Flexible Substrates. *Microsyst. Technol.* **2010**, *16*, 423–430.

- (91) Naghieh, S.; Karamoz-Ravari, M. R.; Sarker, M. D.; Karki, E.; Chen, X. Influence of Crosslinking on the Mechanical Behavior of 3D Printed Alginate Scaffolds: Experimental and Numerical Approaches. *J. Mech. Behav. Biomed. Mater.* **2018**, *80*, 111–118.
- (92) Stowers, R. S.; Allen, S. C.; Suggs, L. J. Dynamic Phototuning of 3D Hydrogel Stiffness. *Proc. Natl. Acad. Sci. U. S. A.* **2015**, *112*, 1953–1958.
- (93) Liu, H.; Li, M.; Liu, S.; Jia, P.; Guo, X.; Feng, S.; Lu, T. J.; Yang, H.; Li, F.; Xu, F. Spatially Modulated Stiffness on Hydrogels for Soft and Stretchable Integrated Electronics. *Mater. Horizons* **2020**, *7*, 203–213.
- (94) Buchberger, A.; Saini, H.; Eliato, K. R.; Zare, A.; Merkley, R.; Xu, Y.; Bernal, J.; Ros, R.; Nikkhah, M.; Stephanopoulos, N. Reversible Control of Gelatin Hydrogel Stiffness by Using DNA Crosslinkers. *ChemBioChem.* **2021**, *22*, 1755–1760.
- (95) Abdeen, A. A.; Lee, J.; Bharadwaj, N. A.; Ewoldt, R. H.; Kilian, K. A. Temporal Modulation of Stem Cell Activity Using Magnetoactive Hydrogels. *Adv. Healthc. Mater.* **2016**, *5*, 2536–2544.
- (96) Díaz-Bello, B.; Monroy-Romero, A. X.; Pérez-Calixto, D.; Zamarrón-Hernández, D.; Serna-Marquez, N.; Vázquez-Victorio, G.; Hautefeuille, M. Method for the Direct Fabrication of Polyacrylamide Hydrogels with Controlled Stiffness in Polystyrene Multiwell Plates for Mechanobiology Assays. *ACS Biomater. Sci. Eng.* **2019**, *5*, 4219–4227.
- (97) Shintake, J.; Schubert, B.; Rosset, S.; Shea, H.; Floreano, D. Variable Stiffness Actuator for Soft Robotics Using Dielectric Elastomer and Low-Melting-Point Alloy. In *IEEE International Conference on Intelligent Robots and Systems*; 2015; pp 1097–1102.
- (98) Shan, W. L.; Lu, T.; Wang, Z. H.; Majidi, C. Thermal Analysis and Design of a Multi-Layered Rigidity Tunable Composite. *Int. J. Heat Mass Transfer* **2013**, *66*, 271–278.
- (99) Shan, W.; Lu, T.; Majidi, C. Soft-Matter Composites with Electrically Tunable Elastic Rigidity. *Smart Mater. Struct.* **2013**, *22*, 085005.
- (100) Ren, L.; Sun, S.; Casillas-Garcia, G.; Nancarrow, M.; Peleckis, G.; Turdy, M.; Du, K.; Xu, X.; Li, W.; Jiang, L.; Dou, S. X.; Du, Y. A Liquid-Metal-Based Magnetoactive Slurry for Stimuli-Responsive Mechanically Adaptive Electrodes. *Adv. Mater.* **2018**, *30*, 1802595.
- (101) Piskarev, Y.; Shintake, J.; Chautems, C.; Lussi, J.; Boehler, Q.; Nelson, B. J.; Floreano, D. A Variable Stiffness Magnetic Catheter Made of a Conductive Phase-Change Polymer for Minimally Invasive Surgery. *Adv. Funct. Mater.* **2022**, *32*, 2107662.
- (102) Wu, Y.; Fang, Z.; Wu, W.; Li, K.; Lin, M.; Dang, Z. Tuning Flexibility-Rigidity Conversion of Liquid Metal/Polyurethane Composites by Phase Transition for Potential Shape Memory Application. *Adv. Eng. Mater.* **2021**, *23*, 2100372.
- (103) Huang, H. W.; Uslu, F. E.; Katsamba, P.; Lauga, E.; Sakar, M. S.; Nelson, B. J. Adaptive Locomotion of Artificial Microswimmers. *Sci. Adv.* **2019**, *5*, No. eaau1532.
- (104) Liu, X.; Kent, N.; Ceballos, A.; Streubel, R.; Jiang, Y.; Chai, Y.; Kim, P. Y.; Forth, J.; Hellman, F.; Shi, S.; Wang, D.; Helms, B. A.; Ashby, P. D.; Fischer, P.; Russell, T. P. Reconfigurable Ferromagnetic Liquid Droplets. *Science* **2019**, *365*, 264–267.
- (105) Huang, H. W.; Sakar, M. S.; Petruska, A. J.; Pané, S.; Nelson, B. J. Soft Micromachines with Programmable Motility and Morphology. *Nat. Commun.* **2016**, *7*, 12263.
- (106) Cowburn, R. P. Property Variation with Shape in Magnetic Nanoelements. *J. Phys. D. Appl. Phys.* **2000**, *33*, R1.
- (107) Zhang, J.; Salehzadeh, M.; Diller, E. Parallel Pick and Place Using Two Independent Untethered Mobile Magnetic Microgrippers. In *Proceedings - IEEE International Conference on Robotics and Automation*; 2018; pp 123–128.
- (108) Gu, H.; Boehler, Q.; Ahmed, D.; Nelson, B. J. Magnetic Quadrupole Assemblies with Arbitrary Shapes and Magnetizations. *Sci. Robot.* **2019**, *4*, No. eaax8977.
- (109) Lin, D.; Wang, J.; Jiao, N.; Wang, Z.; Liu, L. A Flexible Magnetically Controlled Continuum Robot Steering in the Enlarged Effective Workspace with Constraints for Retrograde Intrarenal Surgery. *Adv. Intell. Syst.* **2021**, *3*, 2000211.
- (110) Cowburn, R. P.; Koltsov, D. K.; Adeyeye, A. O.; Welland, M. E.; Tricker, D. M. Single-Domain Circular Nanomagnets. *Phys. Rev. Lett.* **1999**, *83*, 1042–1045.
- (111) Dong, Y.; Wang, L.; Xia, N.; Yang, Z.; Zhang, C.; Pan, C.; Jin, D.; Zhang, J.; Majidi, C.; Zhang, L. Untethered Small-Scale Magnetic Soft Robot with Programmable Magnetization and Integrated Multifunctional Modules. *Sci. Adv.* **2022**, *8*, No. eabn8932.
- (112) Zhou, C.; Yang, Y.; Wang, J.; Wu, Q.; Gu, Z.; Zhou, Y.; Liu, X.; Yang, Y.; Tang, H.; Ling, Q.; Wang, L.; Zang, J. Ferromagnetic Soft Catheter Robots for Minimally Invasive Bioprinting. *Nat. Commun.* **2021**, *12*, 5072.
- (113) Wang, X.; Mao, G.; Ge, J.; Drack, M.; Cañón Bermúdez, G. S.; Wirthl, D.; Illing, R.; Kosub, T.; Bischoff, L.; Wang, C.; Fassbender, J.; Kaltenbrunner, M.; Makarov, D. Untethered and Ultrafast Soft-Bodied Robots. *Commun. Mater.* **2020**, *1*, 67.
- (114) Lee, H.; Kim, J.; Kim, H.; Kim, J.; Kwon, S. Colour-Barcoded Magnetic Microparticles for Multiplexed Bioassays. *Nat. Mater.* **2010**, *9*, 745–749.
- (115) Li, M.; Wang, Y.; Chen, A.; Naidu, A.; Napier, B. S.; Li, W.; Rodriguez, C. L.; Crooker, S. A.; Omenetto, F. G. Flexible Magnetic Composites for Light-Controlled Actuation and Interfaces. *Proc. Natl. Acad. Sci. U. S. A.* **2018**, *115*, 8119–8124.
- (116) Rivkin, B.; Becker, C.; Singh, B.; Aziz, A.; Akbar, F.; Egunov, A.; Karnaushenko, D. D.; Naumann, R.; Schäfer, R.; Medina-Sánchez, M.; Karnaushenko, D.; Schmidt, O. G. Electronically Integrated Microcatheters Based on Self-Assembling Polymer Films. *Sci. Adv.* **2021**, *7*, No. eab15408.
- (117) Bandari, V. K.; Nan, Y.; Karnaushenko, D.; Hong, Y.; Sun, B.; Striggow, F.; Karnaushenko, D. D.; Becker, C.; Faghih, M.; Medina-Sánchez, M.; Zhu, F.; Schmidt, O. G. A Flexible Microsystem Capable of Controlled Motion and Actuation by Wireless Power Transfer. *Nat. Electron.* **2020**, *3*, 172–180.
- (118) Kim, M.; Kim, D.; Aktas, B.; Choi, H.; Puigmarti-Luis, J.; Nelson, B. J.; Pané, S.; Chen, X. Z. Strain-Sensitive Flexible Magnetoelectric Ceramic Nanocomposites. *Adv. Mater. Technol.* **2023**, *8*, 2202097.
- (119) Gu, H.; Möckli, M.; Ehmke, C.; Kim, M.; Wieland, M.; Moser, S.; Bechinger, C.; Boehler, Q.; Nelson, B. J. Self-Folding Soft-Robotic Chains with Reconfigurable Shapes and Functionalities. *Nat. Commun.* **2023**, *14*, 1263.
- (120) Akinyemi, T. O.; Omisore, O. M.; Lu, G.; Wang, L. Toward a Fiber Bragg Grating-Based Two-Dimensional Force Sensor for Robot-Assisted Cardiac Interventions. *IEEE Sensors Lett.* **2022**, *6*, 1–4.
- (121) He, S.; Song, J.; Qu, J.; Cheng, Z. Crucial Breakthrough of Second Near-Infrared Biological Window Fluorophores: Design and Synthesis toward Multimodal Imaging and Theranostics. *Chemical Society Reviews* **2018**, *47*, 4258–4278.
- (122) Zhong, Y.; Dai, H. A Mini-Review on Rare-Earth down-Conversion Nanoparticles for NIR-II Imaging of Biological Systems. *Nano Res.* **2020**, *13*, 1281–1294.
- (123) Zhong, Y.; Ma, Z.; Wang, F.; Wang, X.; Yang, Y.; Liu, Y.; Zhao, X.; Li, J.; Du, H.; Zhang, M.; Cui, Q.; Zhu, S.; Sun, Q.; Wan, H.; Tian, Y.; Liu, Q.; Wang, W.; Garcia, K. C.; Dai, H. In Vivo Molecular Imaging for Immunotherapy Using Ultra-Bright near-Infrared-IIb Rare-Earth Nanoparticles. *Nat. Biotechnol.* **2019**, *37*, 1322–1331.
- (124) Yu, Y.; Nassar, J.; Xu, C.; Min, J.; Yang, Y.; Dai, A.; Doshi, R.; Huang, A.; Song, Y.; Gehlhar, R.; Ames, A. D.; Gao, W. Biofuel-Powered Soft Electronic Skin with Multiplexed and Wireless Sensing for Human-Machine Interfaces. *Sci. Robot.* **2020**, *5*, No. eaaz7946.
- (125) Song, Y.; Min, J.; Yu, Y.; Wang, H.; Yang, Y.; Zhang, H.; Gao, W. Wireless Battery-Free Wearable Sweat Sensor Powered by Human Motion. *Sci. Adv.* **2020**, *6*, No. eaay9842.
- (126) Yoshida, K.; Onoe, H. Soft Spiral-Shaped Microswimmers for Autonomous Swimming Control by Detecting Surrounding Environments. *Adv. Intell. Syst.* **2020**, *2*, 2000095.
- (127) Li, T.; Li, J.; Morozov, K. I.; Wu, Z.; Xu, T.; Rozen, I.; Leshansky, A. M.; Li, L.; Wang, J. Highly Efficient Freestyle Magnetic Nanoswimmer. *Nano Lett.* **2017**, *17*, 5092–5098.

- (128) Magdanz, V.; Sanchez, S.; Schmidt, O. G. Development of a sperm-flagella driven micro-bio-robot. *Adv. Mater.* **2013**, *25*, 6581–6588.
- (129) Medina-Sánchez, M.; Schwarz, L.; Meyer, A. K.; Hebenstreit, F.; Schmidt, O. G. Cellular cargo delivery: Toward assisted fertilization by sperm-carrying micromotors. *Nano Lett.* **2016**, *16*, 555–561.
- (130) Schwarz, L.; Medina-Sánchez, M.; Schmidt, O. G. Sperm-hybrid micromotors: on-board assistance for nature's bustling swimmers. In *Reproduction*; Cambridge, England.
- (131) Xu, H.; Medina-Sánchez, M.; Maitz, M. F.; Werner, C.; Schmidt, O. G. Sperm Micromotors for Cargo Delivery through Flowing Blood. *ACS Nano* **2020**, *14*, 2982.
- (132) Alapan, Y.; Bozuyuk, U.; Erkoc, P.; Karacakol, A. C.; Sitti, M. Multifunctional Surface Microrollers for Targeted Cargo Delivery in Physiological Blood Flow. *Sci. Robot.* **2020**, *5*, aba5726.
- (133) Fan, X.; Dong, X.; Karacakol, A. C.; Xie, H.; Sitti, M. Reconfigurable Multifunctional Ferrofluid Droplet Robots. *Proc. Natl. Acad. Sci. U. S. A.* **2020**, *117*, 27916–27926.
- (134) Zhang, Y.; Jiang, S.; Hu, Y.; Wu, T.; Zhang, Y.; Li, H.; Li, A.; Zhang, Y.; Wu, H.; Ding, Y.; Li, E.; Li, J.; Wu, D.; Song, Y.; Chu, J. Reconfigurable Magnetic Liquid Metal Robot for High-Performance Droplet Manipulation. *Nano Lett.* **2022**, *22*, 2923–2933.
- (135) Miskin, M. Z.; Cortese, A. J.; Dorsey, K.; Esposito, E. P.; Reynolds, M. F.; Liu, Q.; Cao, M.; Muller, D. A.; McEuen, P. L.; Cohen, I. Electronically Integrated, Mass-Manufactured, Microscopic Robots. *Nature* **2020**, *584*, 557–561.
- (136) Utada, A. S.; Lorenceau, E.; Link, D. R.; Kaplan, P. D.; Stone, H. A.; Weitz, D. A. Monodisperse Double Emulsions Generated from a Microcapillary Device. *Science* **2005**, *308*, 537–541.
- (137) Lin, X.; Zhu, H.; Zhao, Z.; You, C.; Kong, Y.; Zhao, Y.; Liu, J.; Chen, H.; Shi, X.; Makarov, D.; Mei, Y. Hydrogel-Based Janus Micromotors Capped with Functional Nanoparticles for Environmental Applications. *Adv. Mater. Technol.* **2020**, *5*, 2000279.
- (138) Zhang, J. M.; Aguirre-Pablo, A. A.; Li, E. Q.; Buttner, U.; Thoroddsen, S. T. Droplet Generation in Cross-Flow for Cost-Effective 3D-Printed “Plug-and-Play” Microfluidic Devices. *RSC Adv.* **2016**, *6*, 81120–81129.
- (139) Deshpande, S.; Caspi, Y.; Meijering, A. E. C.; Dekker, C. Octanol-Assisted Liposome Assembly on Chip. *Nat. Commun.* **2016**, *7*, 10447.
- (140) Zhao, Y.; Xie, Z.; Gu, H.; Jin, L.; Zhao, X.; Wang, B.; Gu, Z. Multifunctional Photonic Crystal Barcodes from Microfluidics. *NPG Asia Mater.* **2012**, *4*, No. e25.
- (141) Akamatsu, K.; Minezaki, K.; Yamada, M.; Seki, M.; Nakao, S. I. Direct Observation of Splitting in Oil-In-Water-In-Oil Emulsion Droplets via a Microchannel Mimicking Membrane Pores. *Langmuir* **2017**, *33*, 14087–14092.
- (142) Akamatsu, K.; Kanasugi, S.; Nakao, S. I.; Weitz, D. A. Membrane-Integrated Glass Capillary Device for Preparing Small-Sized Water-in-Oil-in-Water Emulsion Droplets. *Langmuir* **2015**, *31*, 7166–7172.
- (143) Chen, Y.; Gao, W.; Zhang, C.; Zhao, Y. Three-Dimensional Splitting Microfluidics. *Lab Chip* **2016**, *16*, 1332–1339.
- (144) Liu, Y.; Lin, G.; Chen, Y.; Mönch, I.; Makarov, D.; Walsh, B. J.; Jin, D. Coding and Decoding Stray Magnetic Fields for Multiplexing Kinetic Bioassay Platform. *Lab Chip* **2020**, *20*, 4561–4571.
- (145) Lin, G.; Liu, Y.; Huang, G.; Chen, Y.; Makarov, D.; Lin, J.; Quan, Z.; Jin, D. 3D Rotation-Trackable and Differentiable Micromachines with Dimer-Type Structures for Dynamic Bioanalysis. *Adv. Intell. Syst.* **2021**, *3*, 2000205.
- (146) Xu, C.; Wu, X.; Huang, G.; Mei, Y. Rolled-up Nanotechnology: Materials Issue and Geometry Capability. *Advanced Materials Technologies* **2018**, *4*, 1800486.
- (147) Bandari, V. K.; Schmidt, O. G. System-Engineered Miniaturized Robots: From Structure to Intelligence. *Adv. Intell. Syst.* **2021**, *3*, 2000284.
- (148) Mei, Y.; Solovev, A. A.; Sanchez, S.; Schmidt, O. G. Rolled-up Nanotech on Polymers: From Basic Perception to Self-Propelled Catalytic Microengines. *Chem. Soc. Rev.* **2011**, *40*, 2109–2119.
- (149) Cheng, S.; Hang, C.; Ding, L.; Jia, L.; Tang, L.; Mou, L.; Qi, J.; Dong, R.; Zheng, W.; Zhang, Y.; Jiang, X. Electronic Blood Vessel. *Matter* **2020**, *3*, 1664–1684.
- (150) Li, J.; Li, X.; Luo, T.; Wang, R.; Liu, C.; Chen, S.; Li, D.; Yue, J.; Cheng, S. H.; Sun, D. Development of a Magnetic Microrobot for Carrying and Delivering Targeted Cells. *Sci. Robot.* **2018**, *3*, No. eaat8829.
- (151) Xu, H.; Medina-Sánchez, M.; Schmidt, O. G. Magnetic Micromotors for Multiple Motile Sperm Cells Capture, Transport, and Enzymatic Release. *Angew. Chemie - Int. Ed.* **2020**, *59*, 15029–15037.
- (152) Cabanach, P.; Pena-Francesch, A.; Sheehan, D.; Bozuyuk, U.; Yasa, O.; Borros, S.; Sitti, M. Zwitterionic 3D-Printed Non-Immunogenic Stealth Microrobots. *Adv. Mater.* **2020**, *32*, 2003013.
- (153) De Marco, C.; Pané, S.; Nelson, B. J. 4D Printing and Robotics. *Science Robotics* **2018**, *3*, No. eaau0449.
- (154) Alcántara, C. C. J.; Landers, F. C.; Kim, S.; De Marco, C.; Ahmed, D.; Nelson, B. J.; Pané, S. Mechanically Interlocked 3D Multi-Material Micromachines. *Nat. Commun.* **2020**, *11*, 5957.
- (155) Li, J.; Thiele, S.; Quirk, B. C.; Kirk, R. W.; Verjans, J. W.; Akers, E.; Bursill, C. A.; Nicholls, S. J.; Herkommer, A. M.; Giessen, H.; McLaughlin, R. A. Ultrathin Monolithic 3D Printed Optical Coherence Tomography Endoscopy for Preclinical and Clinical Use. *Light Sci. Appl.* **2020**, *9*, 124.
- (156) Zhang, S.; Hu, X.; Li, M.; Bozuyuk, U.; Zhang, R.; Suadiye, E.; Han, J.; Wang, F.; Onck, P.; Sitti, M. 3D-Printed Micrometer-Scale Wireless Magnetic Cilia with Metachronal Programmability. *Sci. Adv.* **2023**, *9*, No. eadf9462.
- (157) Liu, Y.; Yang, Y.; Yang, X.; Yang, L.; Shen, Y.; Shang, W. Multi-Functionalized Micro-Helical Capsule Robots with Superior Loading and Releasing Capabilities. *J. Mater. Chem. B* **2021**, *9*, 1441–1451.
- (158) Hunter, E. E.; Brink, E. W.; Steager, E. B.; Kumar, V. 3D Micromolding of Small-Scale Biological Robots. In *MARSS 2018 - International Conference on Manipulation, Automation and Robotics at Small Scales*; 2018; pp 1–6.
- (159) Medina-Sánchez, M.; Magdanz, V.; Guix, M.; Fomin, V. M.; Schmidt, O. G. Swimming Microrobots: Soft, Reconfigurable, and Smart. *Adv. Funct. Mater.* **2018**, *28*, 1707228.
- (160) Dabbagh, S. R.; Sarabi, M. R.; Birtek, M. T.; Seyfi, S.; Sitti, M.; Tasoglu, S. 3D-Printed Microrobots from Design to Translation. *Nature Communications* **2022**, *13*, 5875.
- (161) Zhang, C.; Li, X.; Jiang, L.; Tang, D.; Xu, H.; Zhao, P.; Fu, J.; Zhou, Q.; Chen, Y. 3D Printing of Functional Magnetic Materials: From Design to Applications. *Advanced Functional Materials* **2021**, *31*, 2102777.
- (162) Schwarz, L.; Medina-Sánchez, M.; Schmidt, O. G. Hybrid biomicromotors. *Appl. Phys. Rev.* **2017**, *4*, 031301.
- (163) Magdanz, V.; Khalil, I. S. M.; Simmchen, J.; Furtado, G. P.; Mohanty, S.; Gebauer, J.; Xu, H.; Klingner, A.; Aziz, A.; Medina-Sánchez, M.; Schmidt, O. G.; Misra, S. IRONSpERM: Sperm-Templated Soft Magnetic Microrobots. *Sci. Adv.* **2020**, *6*, aba5855.
- (164) Yan, X.; Zhou, Q.; Vincent, M.; Deng, Y.; Yu, J.; Xu, J.; Xu, T.; Tang, T.; Bian, L.; Wang, Y. X. J.; Kostarelos, K.; Zhang, L. Multifunctional Biohybrid Magnetite Microrobots for Imaging-Guided Therapy. *Sci. Robot.* **2017**, *2*, No. eaq1155.
- (165) Gong, D.; Celi, N.; Zhang, D.; Cai, J. Magnetic Biohybrid Microrobot Multimers Based on Chlorella Cells for Enhanced Targeted Drug Delivery. *ACS Appl. Mater. Interfaces* **2022**, *14*, 6320–6330.
- (166) Middelhoek, K. I. N. A.; Magdanz, V.; Abelmann, L.; Khalil, I. S. M. Drug-Loaded IRONSpERM Clusters: Modeling, Wireless Actuation, and Ultrasound Imaging. *Biomed. Mater.* **2022**, *17*, 065001.